UNIVERSITA' DEGLI STUDI DI TRIESTE

XXX CICLO DEL DOTTORATO DI RICERCA IN BIOMEDICINA MOLECOLARE

Role of Mesenchymal Stromal Cells in High-Grade Serous Ovarian Cancer

Settore scientifico-disciplinare: **BIO/11**

DOTTORANDA
Viviana Maria Opinato

Opinato Viviana Maria

COORDINATORE
Prof.ssa Germana Meroni

SUPERVISORE DI TESI
Prof. Claudio Schneider

CO-SUPERVISORE DI TESI
Dott. Roberto Verardo

ANNO ACCADEMICO 2016 / 2017

Summary

Abstract

Mesenchymal Stromal Cells (MSCs) are the precursors of various cell types that compose both normal and cancer tissue microenvironments. In order to support the widely diversified parenchymal cells and tissue organization, MSCs are characterized by a large degree of heterogeneity, although available analysis of molecular and transcriptional data do not provide any clear evidence. Moreover, a wealth of study has demonstrated a significant role of the microenvironment and MSCs in tumor growth. In the laboratory in which I carried out my PhD project, MSCs were purified from different healthy tissues (N-MSCs) and from High-Grade Serous Ovarian Carcinomas (HG-SOC-MSCs). In order to study the role of MSCs in High-Grade Serous Ovarian Cancer, two-dimensional (2D) simplified co-culture approaches were established to characterize the interaction between MSCs and an ovarian carcinoma cell line – Skov3 – at short-term (1 hour) and long-term (5 days) settings. It was demonstrated that short-term co-cultures, specifically performed with transient contact between the two cell types, were able to induce a transcriptional remodeling of Skov3 cells as shown by the up-regulation of ALDH1A3, IL1β, PDPN and MT1E transcripts. Moreover, under the same settings, Skov3 cells co-cultured with HG-SOC-MSCs but not N-MSCs nor when cultured in the presence of HG-SOC-MSCs conditioned medium, were reprogrammed as assessed by specific functional assays, highlighting an increased viability, not linked to proliferation, and higher tumorigenicity and motility. Whole genome expression analysis performed on Skov3 cells subjected to long-term co-culture experiments (5 days), allowed us to focus on different up-regulated transcripts, such as IL8, CXCL1, CXCL2, TNF (involved in the interleukin-10 signaling pathway), CTGF and CYR61 (members of the CCN family), in addition to FOS, EGR1 and ATF4. Such transcripts are significantly up-regulated in Skov3 cells upon direct co-culture with HG-SOC-MSCs, but not or much less with N-MSCs or in membrane-separated co-culture experiments. Furthermore, subcutaneous injection of an admix of Skov3 cells and HG-SOC-MSCs in NOD-SCID mice displayed an

increased kinetics of the Skov3-derived tumor xenograft, showing that HG-SOC-MSCs are able to positively contribute to the tumor growth..

1. Introduction

1.1 Ovarian Cancer

1.1.1 Ovarian cancer is an heterogeneous malignancy

In developed countries, ovarian carcinoma is the most lethal of all gynecologic malignancies (Rauh-Hain et al., 2011)(Siegel et al., 2017). Its high mortality can be attributed to the detection at advanced stage, due to its asymptomaticity (Lowry and Lee, 2017). Overall survival for women with ovarian cancer is 45.6%, but this depends greatly on stage at initial diagnosis (Matulonis et al., 2016). In spite of much work directed to detect an effective tactic for ovarian cancer screening, nowadays there are no screening test recognized to reduce ovarian cancer mortality (Lowry and Lee, 2017) and women with advanced disease display only five-years survival rates (Rauh-Hain et al., 2011).

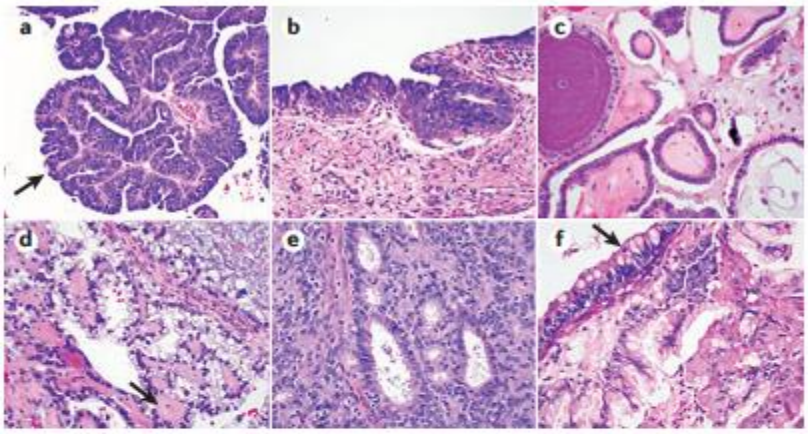

Figure 1 | **Histological subtypes of ovarian cancer. a** | High-grade serous carcinoma (HGSC) is characterized by severe nuclear atypia, high nuclear-to-cytoplasmic ratio and abundant mitoses. Papillary architecture (arrow) is also often present. **b** | Serous tubal intraepithelial carcinoma (STIC) lesions share the same morphological features as HGSC, with severe atypia, mitoses and lack of polarity. STIC lesions are thought to be precursors for HGSC. **c** | Low-grade serous carcinoma (LGSC) shows papillary architecture, but only mild nuclear atypia and a lower nuclear-to-cytoplasmic ratio. **d** | Clear-cell carcinoma is characterized by large atypical tumour cells with frequent clearing of the cytoplasm and stromal hyalinization (arrow). **e** | Endometrioid adenocarcinoma is characterized by gland formation that recapitulates endometrial glands and is graded based on cellular architecture and nuclear atypia. **f** | Mucinous adenocarcinoma shows mucin-filled tumour cells, with frequent goblet cell forms present (arrow).

Figure 1.Matulonis et al., 2016

Recent studies showed that ovarian cancer is a heterogeneous pathology which included various malignant tumors (figure 1) that are distinguishable in terms of etiology, pathogenesis, prognosis, pathology, and molecular pathology (Meinhold-Heerlein and Hauptmann, 2014) and can be subdivided in two main groups: type I and type II. In the first subtype low grade serous cancers, endometrioid and clear cell cancers, and mucinous cancers are included. These cancers have in common a local growth, a late metastasis and mutations in KRAS, ARID1A, PIK3CA, PTEN, and BRAF. The second subtype, instead, is characterized by highly aggressive malignancy, normally present at advanced stage, which is typical of high grade serous cancers, carcinosarcomas, and undifferentiated carcinomas (Terada et al., 2016). The type II is different from the type I also at a genetic level: indeed, the second group displays mainly mutations associated with TP53 (Kurman and Shih, 2011).

1.2 High grade serous ovarian cancer

1.2.1 Genetic characterization

Among all the subtypes aforementioned, high-grade serous ovarian cancer (HG-SOC) is the most frequently diagnosed (Matulonis et al., 2016). As already cited, it is genetically characterized mainly by mutations in TP53, which can occur both in the region of the gene encoding the DNA-binding domain and in regions encoding the non-DNA-binding domains. There are also tumors that, although do not display any TP53 mutations, present an augmented copy number of MDM2 or MDM4. The gene products of MDM2 and MDM4 are involved in the regulation and degradation of p53 (Ahmed et al., 2010).

Moreover, in approximately 50% of HG-SOC cases, defects in homologous recombination were detected (Alsop et al., 2012) (Zhang et al., 2011) which are generally related to both germline and somatic BRCA mutations, along with alterations in genes involved in other DNA repair pathways (Kindelberger et al., 2007)

Besides, further frequent impairment typical of this kind of tumor include defective Notch, phosphoinositide 3-kinase (PI3K), RAS–MEK and forkhead box protein M1 (FOXM1) signaling pathways (Bell et al., 2011). Other genes that, once mutated, can have a role in the pathogenesis of ovarian cancer and could be considered as potential therapeutic targets are AURKA, ERBB3, CDK2, MTOR, BRD4 and MYC (Bell et al., 2011)(Baratta et al., 2015)

1.2.1 Origin site

Lately, it is has been discovered that not all ovarian cancers originates from ovary; indeed, most tumors arise from cells that normally are present in extra-ovarian tissue (Karnezis et al., 2016).

Numerous marks can indicate whether the ovary is the primary site of origin of an ovarian tumor or not. Among these evidences the most remarkable are:

1) anatomical evidence such as the presence of a solitary intra-ovarian tumor,

2) phenotypic evidence such as histological and immune-phenotypic correspondences between a tumor and a normal ovarian cell type,

3) biological evidence like, for example, the capability of normal ovarian cells to be mutated and to summarize the hallmarks of cancer (Hanahan and Weinberg, 2011) (figure 2) in an experimental system and

4) circumstantial evidence, according to which similar tumors in the ovary and testis could indicate an intra-gonadal origin from the analogous cells present in each gonad (Karnezis et al., 2016) .

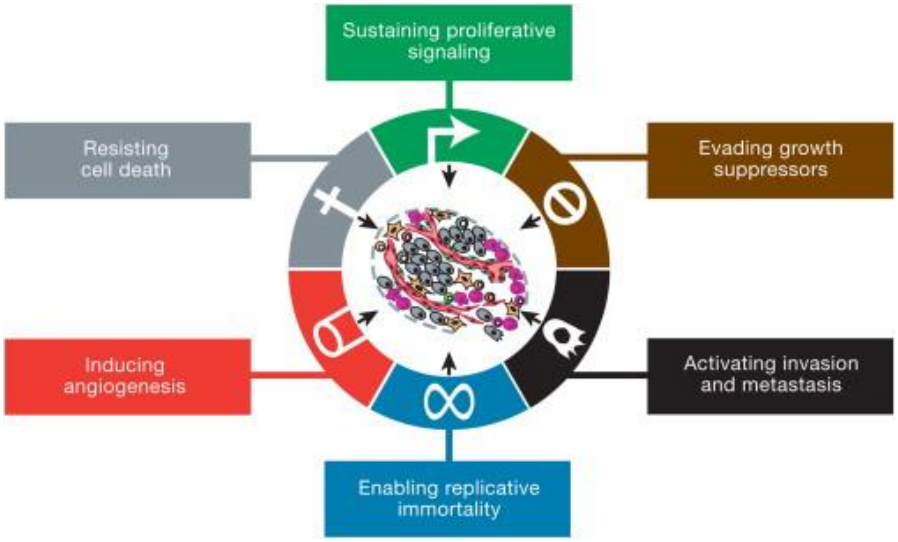

Figure 2. Hanahan and Weinberg, 2011

If these criteria are not satisfied, probably the ovarian tumor originates from cells that normally are not present in the ovary, but can be involved in ovary development. For example, high-grade serous ovarian cancer (HG-SOC) derives from fallopian tubes and this is probably due to the presence of atypical tubal epithelial cells found in patients with mutations in BRCA1 or BRCA2. (Kindelberger et al., 2007).

The discovery of this precursor site has not been easy and it dates back to not so many years ago.

The initial hypothesis was that HG-SOC could arise from an"incessant ovulation". In fact, according to this old hypothesis, continuous "rupture and repair" events of the ovarian epithelium could result into an augmented proliferation, metaplasia of the ovarian surface epithelium (OSE) to a Müllerian phenotype and into damaging mutations that could give rise to this peculiar cancer.(Fathalla, 1971). In 1999, Dubeau proposed the Müllerian epithelium, rather than the OSE, as the original site of these cancers .(Dubeau, 1999)

Finally, fallopian tubes were identified as precursor site thanks to the introduction of a surgery technique called bilateral salpingo-oophorectomy, used to remove ovaries and both fallopian tubes in patients with germline mutations in BRCA1 and BRCA2.(Tone et al.,

2012). It was detected serous tubal intraepithelial carcinoma (STIC) — an early lesion — in the fallopian tubes of women with ovarian cancer at advanced-stage. Moreover, the precursor sites in the fallopian tube were identified by DNA damage and mutations in TP53 (Kindelberger et al., 2007) (Kurman and Shih, 2010) (Medeiros et al., 2006) (Carlson et al., 2008) (Perets et al., 2013) (Lee et al., 2007) (Howitt et al., 2015) (Crum et al., 2013).

Another possible site of HG-SOC recently emerged is fimbriae, the protrusions at the distal end of the fallopian tube next to the ovary.(Gilks et al., 2015)(Morrison et al., 2015).

As already explained above, cancers that do not originate from normal ovarian cell types can present as dominant ovarian masses. Most likely, this occurs because ovary possesses an optimal environment for cancerous and precancerous lesions. At contrary, fallopian tubes appear to have an inhospitable microenvironment for both primary tumors and metastasis (McDaniel et al., 2015) (Rabban et al., 2015) (Reyes et al., 2015). A possible theory to explain why the microenvironment of fallopian tubes is so tumor-suppressive can be that it has the role to avoid ectopic pregnancy; in fact, cancer progression can be promoted by the microenvironment of ovary, but inhibited by the fallopian tube microenvironment. It was hypnotized that microenvironments of the ovary, fallopian tube and peritoneum have distinct roles in tumor initiation, progression and/or growth (figure 3) and that ovarian cells can secrete factors able to allow the implantation, growth and invasion of neoplastic cells. The observation that the fallopian tube mucosa allow the initiation (STIC) or the implantation (HG-SOC and extra-ovarian metastases) of ovarian cancer cells, but do not promote the growth of the tumor as dominant mass, points to the fact that fallopian tube stroma, but not the epithelium, do not permit – directly or indirectly – the tumor progression, at least when related to the ovary. (Karnezis et al., 2016)

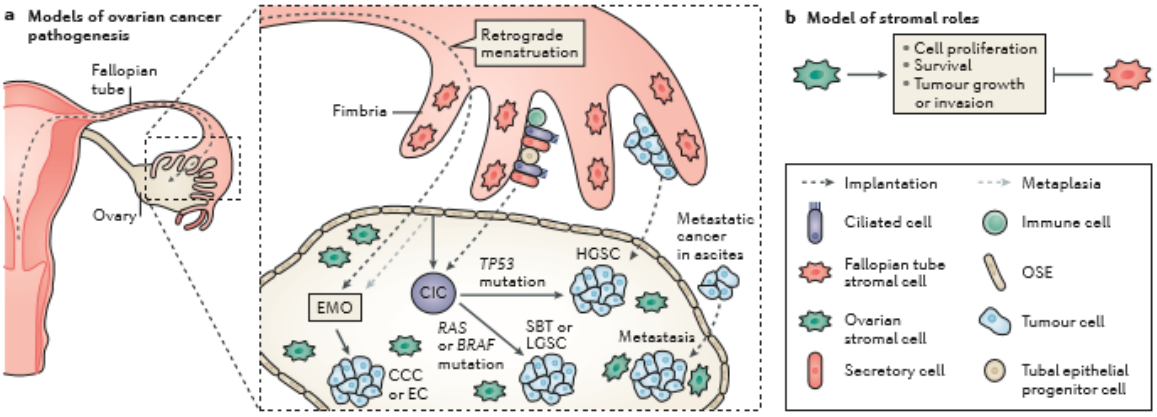

| Microenvironments of the ovary versus fallopian tube in tumour biology. The ability of primary ovarian carcinomas and metastatic carcinomas to grow as large masses in the ovary but not in the fallopian tube mucosa suggests a stimulatory role of ovarian stroma and inhibitory role of fallopian tube stroma in the progression of cancer precursor lesions and growth and/or invasion of cancer cells. Most high-grade serous carcinomas (HGSCs) arise from precursors in the fallopian tube fimbria that are called serous tubal intraepithelial carcinoma, which are thought to implant on the ovary and present as 'ovarian' HGSC, similar to metastatic carcinoma cells in ascites fluid (part **a**). Alternatively, some HGSCs may arise from intra-ovarian tubal epithelium, that is, ovarian endosalpingiosis, also called tubal-type cortical inclusion cysts (CICs). It is unclear whether CICs form by implantation of fimbrial epithelium or by metaplasia of ovarian surface epithelium (OSE). Larger tubal-type CICs are also thought to be an origin of serous borderline tumour (SBT) and low-grade serous carcinoma (LGSC). Ovarian endometriosis (EMO) is thought to arise by retrograde menstruation, by metaplasia or from Müllerian developmental remnants (not depicted). Although EMO is very common, it can acquire mutations and develop into clear cell carcinoma (CCC) or endometrioid carcinoma (EC). The propensity of all these tumours to grow as large ovarian masses rather than tubal masses supports the hypothesis that the ovarian stroma and fallopian tube stroma have stimulatory and inhibitory roles, respectively, in several aspects of tumorigenesis (part **b**). Dashed lines indicate processes or sources of cells (metaplasia or implantation from detached tubal cells, retrograde menstruation or ascites fluid). Solid lines indicate progression (EMO to CCC or EC; possible progression of tubal CIC to HGSC, SBT or LGSC).

Figure 3. Karnezis et al., 2016

1.3 Cancer microenvironment

1.3.1. Cancer cells alone are not sufficient to sustain tumor progression

Conventionally, the focus on the study of tumor initiation, progression and metastasis has been positioned on neoplastic cells. This suggests that alterations in oncogenes and onco-suppressor genes results in aberrations of growth signaling pathways finally leading to uncontrolled cancer cells proliferation. Nevertheless, even though these pathways are fundamental for the metastatic transformation of cells, the unrestrained proliferation of cancer cells cannot be only reconnected to mutations in cancer cells themselves. Tumors are

complex organs compounded of neoplastic cells and stroma, which is in turn composed by blood cells, lymphoid vessels, nerves, stromal cells, extracellular matrix (ECM) proteins, endothelial cells, pericytes and immune cells (figure 4) (Junttila and de Sauvage, 2013) (Cuiffo and Karnoub, 2012) (Hanahan and Weinberg, 2011). Although cancer cells are the ones that cause the "initial insult", tumor microenvironment (TME) forms the tumor niche that co-evolve with neoplastic cells and participate to the tumorigenesis (Junttila and de Sauvage, 2013).

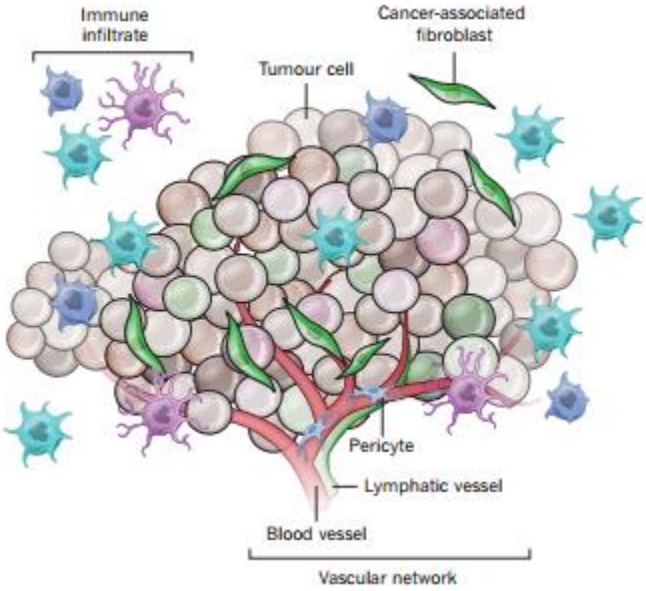

Figure 4. (Junttila and de Sauvage, 2013).

Then, in order to truly understand the tumor behavior, it is fundamental to take in consideration the surrounding environment to which neoplastic cells belong. Indeed, the tumor cells can establish a crosstalk with their stroma that is known to be central for the tumor initiation and progression (Pietras and Östman, 2010), thanks to the stimulated synthesis of cytokines, chemokines, growth factors and proteinases (Junttila and de Sauvage, 2013).

It is possible to resume the types of cells included in TME in three main categories: 1) infiltrating immune cells, 2) angiogenic vascular cells and 3) cancer-associated fibroblastic cells (CAFs) (Hanahan and Coussens, 2012).

1. Generally, the immune system works in order to recognize and protect the organism from insults. In tumors, the innate and adaptive immune systems can play a role both in the promotion and in the prevention of cancer progression. In fact, immune cells have the capacity to mount antitumor responses, but this effect could be abolished by an immune suppressive action. CAFs-secreted factors, the state of the vasculature and tumor cells themselves are elements that strongly influence the heterogeneity in immune tumor environment (Junttila and de Sauvage, 2013). For example, the vascular tumor context is an element that affect the immune state since endothelial cells orchestrate immune cells migration. Ovarian cancers, indeed, possess an unique endothelial transcriptional signatures that resulted in a high percentage of tumor-infiltrating lymphocytes (Buckanovich et al., 2008). Conventionally, the activation of T-cells goes through both stimulatory and inhibitory checkpoint signals in order to tune inflammatory responses and avoid unnecessary injury and autoimmunity. There are two ways to avoid an antitumor action of T cells: the direct and the indirect way. The first one calls for the secretion of inhibitory receptors on T-cells surface, such as cytotoxic T-lymphocyte-associated antigen-4 (CTLA-4) and programmed death 1 (PD1), through an upregulation of their ligands (Pardoll, 2012). The second way concerns the creation of an immunosuppressive environment with the preventing task of antitumor T-cell responses. This immunosuppressive environment can be generated through the expansion of a myeloid-derived suppressor cell population (MDSC), comprehensive of neutrophils, immature dendritic cells, monocytes and early myeloid progenitors. The expansion of MDSCs occurs thanks to an endocrine communication between tumor and CAFs secretion of chemokines such as granulocyte–macrophage colony stimulating factor, (GM-CSF) or granulocyte colony stimulating factor (G-CSF) (Shojaei et al., 2009) (Pylayeva-Gupta et al., 2012) (Bayne et al., 2012). MCDCs not only suppress adaptive immunity, but encourage angiogenesis since an increased

production of VEGFA, basic fibroblast growth factor (bFGF) and transforming growth factor β (TGF-β) occurs (Motz and Coukos, 2011). In addition, MDSCs are able to dump natural killer cell function and to enlarge the immunosuppressive regulatory T-cell population. Moreover, MDSCs can directly play a negative role on effector T-cell increase number, activation and migration (Gabrilovich et al., 2012). Other immune cells such as B cells can both suppress and support T-cell function, resulting in differential effects on tumorigenesis, depending on the contexts (Nelson, 2010). Moreover, independently on T-cell role, different studies have reported that B cells can foster cancer progression by promoting a pro-tumoral inflammation environment (de Visser et al., 2005) (Ammirante et al., 2010). Moreover, mast cell are involved in tumorigenesis and angiogenesis (Coussens et al., 1999) (Yang et al., 2008). Last but not least, tumor-associated macrophages (TAMs) have been reported to influence tumor progression, according to their polarization (Dotto et al., 1988).

2. The tumor vascular network is dynamic and can affect the tumor growth. The formation of new vessels (angiogenesis), the remodeling of the existing tissue vessels together with vasculogenesis define the tumor heterogeneity (Hanahan and Coussens, 2012). Furthermore, vessels generation implicates degradation and remodeling of present vascular basement membranes that are tissue-dependent (Kalluri, 2003). Different levels in vascularization and an ineffective drainage caused by an insufficient lymphatic vessel coverage cooperate to give a complex topography to the tumor. A scarce organization of tumor vasculature results in hypoxia and inadequate nutrient source for some tumor districts. Such alterations in vascular systems can cause different microenvironments within the tumor and "contribute to inter- and intra-tumor heterogeneity", and finally affect the clinical outcome (Junttila and de Sauvage, 2013). For example, microvessel density is nowadays considered one relevant prognostic factor for poor outcome for tumors such as non-small-cell lung cancer (NSCLC) (Meert et al., 2002), colorectal (Des Guetz et al., 2006) and breast (Uzzan et al., 2004) cancer. Moreover, it has been noticed that high level of VEGFA are linked

to a worse prognosis when compared to prognosis characterized by low expression of VEGFA in metastatic colorectal, lung and renal cell cancers (Hegde et al., 2013).

3. In normal contests, fibroblasts are a plentiful mesenchyme-derived cell type that conserve the structural scaffold in tissues by responding, for example, to damage, such as wounding, and becoming triggered to support healing. Generally, normal fibroblasts inhibit tumor generation (Dotto et al., 1988); CAFs, instead, are known to encourage cancer formation (Orimo et al., 2005). To this group of cells belong connective tissue fibroblasts that are triggered by cancer progressions and mesenchymal progenitors—in particular, mesenchymal stem cells (MSCs), both local and bone marrow derived. MSCs can be recruited and prompted to differentiate into myo-fibroblasts that can be partially identified by the marker alpha smooth muscle actin (αSMA) (Paunescu et al., 2011), into adipocytes, expressing fatty acid binding protein-4 (FABP4) (Hanahan and Coussens, 2012) or into chondrocytes and osteocytes. There is another hypothesis according to which CAFs derive from MSCs. This theory born from the evidence that MSCs and CAFs share many similarities. Indeed, they display the same surface markers such as CD29, CD44, CD73, CD90, CD106 and CD117, possess the ability to differentiate to osteocytes, chondrocytes and adipocytes (as described above), and express vimentin (Paunescu et al., 2011). In a work, Kalluri suggested that fibroblasts are quiescent mesenchymal cells that can be activated and can differentiate into MSCs, if stimulated properly (Kalluri, 2016). However, CAFs unveiled an augmented proliferative potential and secrete higher levels of VEGF, TGF-β, IL-4, IL-10 and tumor necrosis factor-α (TNF-α) compared to MSCs (Paunescu et al., 2011). The activation or differentiation mechanisms of CAFs are still widely not known, but it seems that TGF-β is the factor that stimulate phenotypic alterations unrelatedly from cell sources (Zeisberg et al., 2007) (Kojima et al., 2010) (Calon et al., 2014) (Shangguan et al., 2012). When related to fibroblasts derived from normal tissue, CAFs display augmented proliferation, an increased production of extracellular matrix and a peculiar secretion of cytokines, such as stromal cell-derived factor 1 (SDF), vascular endothelial growth factor (VEGF),

platelet-derived growth factor (PDGF) and hepatocyte growth factor (HGF) (Polanska and Orimo, 2013), IL-4, IL-10 and TGF-β (Paunescu et al., 2011). Fibroblast behavior can affect tissue remodeling through an increased expression of specific proteolytic enzymes, such as matrix metalloproteinases, deposition of extracellular matrix and angiogenesis thanks to the release of proangiogenic elements in the matrix (Hanahan et al., 2000). Plasticity of these peculiar kind of cells can be due to the exposition of exclusive damage signals and also to their origin (Quante et al., 2011). Other characteristic of this cell line that increase stromal heterogeneity are the ability to perform both mesenchymal-to-epithelial transitions and epithelial-to-mesenchymal transitions. Even though specific markers have not been identified nowadays, CAFs are clinically significant in a tumor contest. For example, the plenty of stromal cells correlates with poor prognosis for several types of tumors, such as breast (Yamashita et al., 2012) and pancreatic (Fujita et al., 2010) cancer. Moreover, high levels of matrix metalloproteinases associates with augmented aggressiveness and poor prognosis in specific cancers (Vihinen and Kähäri, 2002)

However, recent studies highlighted that some stromal elements can regulate immunosuppression and restrained carcinogenesis, unveiling antitumor activities, at least form some type of cancer such as pancreatic ductal adenocarcinoma (Rhim et al., 2014).

The image below (figure 5) is representative for the roles carried out by the three groups of cells described above.

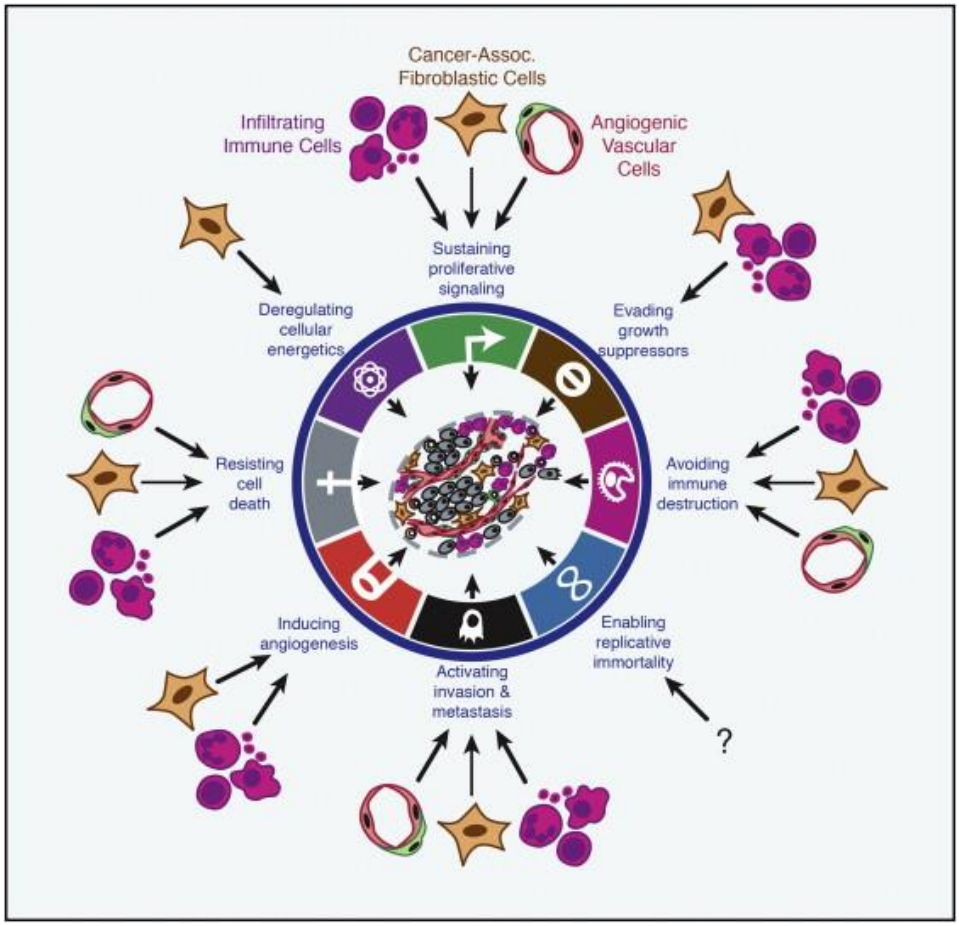

Figure 5. (Hanahan and Coussens, 2012)

1.3.2 MSCs are fundamental actors in tumor progression: introduction to MSCs

As already stated, cancer cells alone are not sufficient to promote tumor condition; indeed, the interaction between neoplastic cells and the adjacent stroma guides to an 'activated state' of the stromal cells which leads to an augmented release of pro-inflammatory cytokines and growth factors (Pietras and Östman, 2010). The tumor is a complex organ that displays a

chronic condition of inflammation and has been defined as a ‘wound that never heals’ (Dvorak, 2015). This state beckons receptive cell types such as macrophages, myeloid derived suppressor cells and mesenchymal stem cells (MSCs) in the inflammatory sites (Pollard, 2004), (Hall et al., 2007a) (Young and Wright, 1992). It has been reported that cross-talk between neoplastic cells and cells from the adjacent stroma can encourage cancer progression and generates a dynamic ECM, which promotes cancer invasiveness (Sato et al., 2004) (Sung et al., 2008). What makes the study of the interaction between tumor cells and the relative stroma difficult is that the stroma is peculiar for each kind of cancer, and cancer itself display a heterogeneous nature. Thus, it becomes fundamental to acquire a knowledge about what stimulates non-cancerous cells toward an “activated state” and what this means for cancer progression (Ridge et al., 2017).

In this work, I focused the attention on a peculiar kind of stromal cells: MSCs.

MSCs are multipotent stem cells characterized by the ability to differentiate into the three cell types: osteoblasts, chondrocytes and adipocytes (Pittenger et al., 1999) and by positivity for surface markers like CD73, CD105 and CD90 (Dominici et al., 2006). Recently, it has been reported that MSCs can differentiate also in neurons, myocytes and myo-fibroblasts, showing a broader differentiation potential (Wakitani et al., 1995) (Kopen et al., 1999). Generally, the principal sources of MSCs are the bone marrow, adipose tissue and dental pulp (Pittenger et al., 1999) (Gronthos et al., 2000) (Huang et al., 2002) (Friedenstein et al., 1970); however, they are also present in circulation and, indeed, they can home to inflammatory sites (Chamberlain et al., 2007). MSCs might be recruited to damaged tissues by inflammatory cytokines and chemokines in order to collaborate in tissue regeneration and repair (Sun et al., 2014). During this event, MSCs contact several kind of cells through two possible ways:

1) either by the extracellular vesicles (EV) release that express bioactive molecules (such as for example proteins, lipids, and RNA) which can have an anti-inflammatory or anti-tumoral role (Caplan and Correa, 2011) (Katsuda et al., 2013) or 2) by direct cell–cell contact via integrins and intercellular gap junctions (Ruster et al., 2006).

Given their ability to migrate and home to damaged tissues, there are many studies that proposed a reparative role for MSCs in different tissues such as the lung (Ortiz et al., 2003), liver (Sato et al., 2005), brain (Ji et al., 2004) and heart (Wu et al., 2003).

Moreover, MSCs help as niche for further cell kinds, by orchestrating regenerative processes. Undeniably, they have a role in both hematopoietic cells growth and hematopoietic stem cells (HSCs) regulation (Krosl et al., 2003) (Zhang et al., 2006) (Willert et al., 2003) (Butler et al., 2010). In particular, they participate to HSCs self-renewal and differentiation by directing the osteogenic niche (Arai et al., 2004) (Calvi et al., 2003) (Zhang et al., 2003) (Kollet et al., 2006). Because of all these capacities and characteristics, MSCs appear to be an interesting target for regenerative medicine and for therapeutics use in cardiology, immunology and neurology fields.

Nevertheless, many researches in tumor field propose a correlation between MSCs and poor outcomes (Ame-Thomas et al., 2007) (Kansy et al., 2014) (Karnoub et al., 2007) (Prantl et al., 2010a).
Indeed, recent studies showed that MSCs can also home to tumor sites, promoting tumor development and progression (Karnoub et al., 2007) (Prantl et al., 2010a) (Kucerova et al., 2010) (Suzuki et al., 2011). Interestingly, prostate tumors have been analyzed upon prostatectomies and a percentage of 0.01-1.1% of MSCs has been quantified on total cells (Brennen et al., 2013). Furthermore, MSCs play an important role in cancer metastasis. Indeed, MSCs can augment metastatic potential through the stimulation of their motility and invasiveness not forgetting their part in the generation of a metastatic niche at the secondary site (Karnoub et al., 2007) (Nabha et al., 2008) (Duda et al., 2010) (Corcoran et al., 2008).
The association between MSCs and tumor progression have been noticed in different kind of cancers: like, for example, follicular lymphoma (Ame-Thomas et al., 2007), head and neck carcinoma (Kansy et al., 2014), glioma (Hossain et al., 2015), breast (Karnoub et al., 2007), gastric (Li et al., 2015), colon (Zhu et al., 2006) and prostate cancer (Prantl et al., 2010a). Moreover, it has been demonstrated that co-injection of MSCs derived from bone marrow (BM-MSCs) with MCF7, a breast cancer cell line, into mice drove to an increased speed of

tumor growth and that the co-injection with four breast cancer cell lines all together encouraged an augmented metastasis (Karnoub et al., 2007).

Likewise, a recent study demonstrated that co-injection of human BM- MSCs with SUM149, a triple negative breast cancer cell line, led to a dumped primary tumor progression, but to an augmented invasion and metastasis in mice (Lacerda et al., 2015). These conclusions suggest that MSCs could promote metastasis at the tumor site, perhaps owing to the stimulation of epithelial-to-mesenchymal transition (EMT) in primary tumor cells (Ridge et al., 2017). Co-injection of MSCs derived from human adipose tissues and MDA-PCa-118b (a prostate cancer cell line) in mice unveiled an augmented tumor growth.(Prantl et al., 2010b). In a different research, the proliferative, migration and invasiveness potential of prostate cancer cell line PC3 was encouraged by bone marrow MSCs *in vitro*. This increase was repressed when TGFβ was blocked (Ye et al., 2012). Growth factors and cytokines are dualistic players in cancer and TGFβ does not make any exception. TGFβ, indeed, appears to be an oncosuppressor in the early stage of carcinogesis, but in the late tumor phases it can encourage the metastasis, by promoting EMT (Costanza et al., 2017). Interesting it is that colorectal cancer needs stromal derived TGFβ to initiate metastasis (Calon et al., 2012).

Another interesting approach through which the role of MSCs within the tumor microenvironment has been studied was to isolate MSCs from tumor. Remarkably, injection of MSCs derived from human head and neck carcinoma (Kim et al., 2013), gastric cancer (Kansy et al., 2014) and gliomas (Hossain et al., 2015) together with tumor cells in mice led to an increase cancer development and evolution, respectively. Finally, it was discovered that MSCs isolated from tumors, such as human gastric, encouraged *in vitro* augmented proliferation and migration of gastric cancer cell lines, such as BGC-823 and MKN-28, when related to MSCs isolated from bone marrow or non-cancerous adjacent tissue. It was also noticed that cancer-derived MSCs were able to secrete a greater level vascular endothelial growth factor (VEGF), macrophage inflammatory protein-2, TGF-β and the pro-inflammatory cytokines interleukin IL-6 and IL-8. Moreover, inhibition of IL-8 resulted in a diminished tumor promoting ability of the gastric cancer-derived MSCs (Li et al., 2015)

It has to be reported that MSCs functions are deeply different and strongly correlated to their source. Indeed, MSCs isolated from the bone marrow, adipose tissue and dental pulp are not functionally identical and can give different results (Lee et al., 2004), (Wagner et al., 2005). This can be linked to the evidence that some MSCs can possess a tumor suppressive role. For example, a system of implanted human MSCs, isolated from the umbilical cord and adipose tissue, into a breast cancer metastasis mouse model displayed a decreased metastasis to the lung and a dumped cancer growth via poly (ADP-ribose) polymerase (PARP) and caspase-3 cleavage, that could in turn promote apoptosis (Sun et al., 2009). This has not to be surprising because MSCs are a various population of cells that include subpopulations with heterogeneous differentiation capacities (Horwitz et al., 2005). Indeed, MSCs can express embryonic stem cell or pluripotency markers that varied in relation to the source. For example, MSCs isolated from bone marrow express Oct4, Nanog, alkaline phosphatase and SSEA-4, adipose and dermis derived MSCs present high levels of Oct4, Nanog, SOX2, alkaline phosphatase and SSEA-4; while heart MSCs display Oct4, Nanog, SOX2 and SSEA-4 (Riekstina et al., 2009). It has to be considered that the molecular and phenotypic characterization of MSCs strongly depends on the technique used to isolate them, even though the major markers identified remained CD105 and CD90. Indeed, different isolation techniques and growth conditions can promote the development of certain subpopulations despite others (Karnoub et al., 2007) (Lacerda et al., 2015) (Ye et al., 2012) (Sun et al., 2009) (Otsu et al., 2009) (Spaeth et al., 2009) (Mishra et al., 2008) (Shangguan et al., 2012). Furthermore, it was demonstrated that MSCs isolated from murine bone marrow displayed a cytotoxic effect on a murine melanoma via the release of ROS when interacting with endothelial cells (ECs), at the capillaries sites. This effect led to the apoptosis of ECs and a reduction in the tumor expansion. However, the cytotoxicity was found only when MSCs were implanted with an EC/MSCs ration of 1:1 or 1:3. The effect diminished notably when the number of MSCs implanted was decremented by an order of magnitude (Otsu et al., 2009). These observation can clarify the apparent discrepancy with the results displaying that MSCs can promote tumor growth: when the MSCs effect on tumor biology are analyzed, the

origin of MSCs and the specific cell ratio MSCs/tumor cells have to be take in consideration because they are conditions that may reflect the physiological tumor environment.

In addition, another reason for the opposing outcomes is that, like in the case of macrophages, there is a polarization of MSCs depending on tumor secreted factors that can either pushes the cells to a tumor supporting or suppressive function. According to the stimuli, macrophages can be polarized toward an M1 or M2 phenotype. The M1 phenotype is normally stimulated by interferon gamma (IFN-γ) and lipopolysaccharides (LPS). It displays cytotoxic effects on tumor cells. On the contrary, M2 macrophages are prompted by IL-4, IL-13 and IL-10 and they support wound healing and angiogenesis. Moreover, M2 macrophages are phenotypically similar to TAMs (Mantovani et al., 2002) (Allavena et al., 2008) (Sica et al., 2006).

Interestingly, it has been reported formerly that MSCs can express toll-like receptor (TLR)-1, 2, 3, 4, 5 and 6 and TLR-agonist interaction encouraged specific MSCs functions such migration and secretion of immunomodulatory factor (Tomchuck et al., 2008). In particular, LPS stimulated-TLR4 and Poly-IC stimulated-TLR3 led to augmented levels of phospho-IKKα/β and phospho-MAPK, respectively. This indicates that activation of TLR4 or TLR3 may orchestrate NFkB and/or MAPK signaling in MSCs. Moreover, TLR4 activation resulted also into a higher expression level of IL-6 and IL-8 (Tomchuck et al., 2008). Notably, Waterman and colleagues suggested that MSCs could polarize depending on TLR signaling. The authors discovered discrepancies at functional level between MSCs isolated from human bone marrow stimulated by either TLR4 or TLR3 and identified them as MSC1 and MSC2, respectively (Waterman et al., 2010). The principal difference is that MSC1 cells display an anti-tumor effect and MSC2 cells, instead, support tumor growth and metastasis (Waterman et al., 2012). These results can have a clinical relevance. Indeed, since high levels of both TLR3 and TLR4 in breast tumor epithelium correlated with augmented risk of disease recurrence (González-Reyes et al., 2010), and taken in the context of their promoting and suppressive tumoral effects in MSCs (Waterman et al., 2012), it appears clear that targeting TLRs for tumor treatment is intricate. In fact, the benefits of this therapeutic treatment can depend on the specific polarization of MSCs and immune cells in the tumor

microenvironment; not forgetting also the TLR expression patterns within the tumor epithelia in each single patient.

1.3.2 MSCs and Ovarian Cancer

In ovarian cancer, the communication between tumor and stromal cells drives to "bilateral phenotype modulation". Indeed, a part from the phenotypic modifications that occur in Ovarian Cancer Cells (OCCs), it has been observed that also the phenotype of cancer-associated MSCs can change (Touboul et al., 2014). Though it may vary depending on the kind of cancer, the alteration in MSCs phenotype upon their homing into neoplastic stroma typically leads to tumorigenesis promotion. The pro-oncogenic modification in MSCs phenotype is orchestrated, at least in part, by factors secreted from tumor.

For example, lysophosphatidique acid (LPA) is a small bioactive phospholipid secreted by OCCs that promotes differentiation of MSCs in myofibroblast-like cells (Cai and Xu, 2013) (Jeon et al., 2008) (Direkze et al., 2004). As already explained previously, these cells are included in a group of cells called CAFs, which are a keystone in the formation of tumor microenvironment.

The mechanism through which MSCs engraft in tumor stroma, by shifting toward a CAFs-like phenotype, may implicate exosomes secreted by the tumor (Cho et al., 2011). Fascinatingly, exosomes from diverse ovarian cancer cell lines (Ovcar3 and Skov3) stimulate different MSCs signaling pathways (SMAD and AKT, respectively). This proposes that exosome content may differ depending on cancer cell phenotype and orchestrating, at least in part, the tumor stroma consequently. Moreover, a genomic approach also associates OCCs capacity to prompt CAFs features in MSCs through the expression of HOXA9, a Mullerian-patterning gene (Ko et al., 2012). HOXA9 expression leads to high transcriptional levels of TGFβ2 that stimulate MSCs to express IL-6, VEGF-A and SDF1. It has also been described a process through which OCCs secrete IL-1β, instructing a CAFs niche by suppressing p53

(Schauer et al., 2013a). Consequently, the CAFs niche secretes IL-8, growth regulated oncogene-alpha (GRO-α), IL-6 and VEGF. Hence, the MSCs phenotype modulation helps in the creation of a "cytokine mediated inflammatory contexture" appropriate for tumor development (Touboul et al., 2014).

Additionally, once MSCs shift toward CAFs they collaborate to form the tumoral fibrovascular networks (Spaeth et al., 2009) (Hall et al., 2007b). CAFs not only enrich the perivascular matrix with desmin and α-SMA (Spaeth et al., 2009), but they also secrete versican, a large ECM proteoglycan. TGFβ via TGFβ-RII and SMAD signaling maintain high level of (Yeung et al., 2013) versican that promotes OCCs motility. OCCs express also metalloprotease MMP-3 that contributes to ECM regulation (Spaeth et al., 2009) and to stromal alterations, leading to tumor expansion, encouraged at the same time by CAFs secretion of HGF, EGF, IL-6 and SDF1, which support the tumor growth (Hall et al., 2007b). In ovarian cancer, high levels of SDF1 are expressed both by CAFs and OCCs. SDF1 contributes to the microenvironment development of the tumor and stimulates tumor growth through different mechanisms. First, it exerts a local immunity suppressive function by recruiting plasmacytoid dendritic cell precursors that drive to the triggering of poor anti-tumoral T cells, via the up regulation of IL-10 and TNFα (Zou et al., 2001) (Scotton et al., 2002). SDF1 also interacts with CXCR4, consequently trans-activates EGFR and promotes a dose-dependent OCCs proliferation (Porcile et al., 2005). SDF1 possesses also other roles in this context such as: contributes to adhesion and migration of cancer cells by instructing MAP and Akt kinase (Kukreja et al., 2005) (Peng et al., 2005); stimulates angiogenesis at tumor sites (Kryczek et al., 2005) and functions as a chemo attractant for endothelial progenitor cells (EPCs) positive for CXCR4 (Orimo et al., 2005)

Moreover, it is a well-known fact that certain tumor types metastasize to determined organs. In particular, ovarian cancer is organized in order to spread only into designated organs. In addition to the capacities of cancer cells, the tumoral surrounding environment together with the local stroma cells of distant sites collaborate in this process. The resident stromal cells of the pre-metastatic niche, indeed, recruit hematopoietic progenitor cells (HPCs) by secreting fibronectin, an adhesion protein inducing VLA-4 (integrin α4β1) (Kaplan et al., 2005). α4β1

signaling contributes to alteration in the local ECM through MMP-9. The recruiting of HPCs VEGFR1+ from the microenvironment modifications results in a pre-metastatic scenario via a cytokine system, involving TNFα, MMP-9, TGFβ, and SDF1 (Psaila and Lyden, 2009).

Although different tumors possess a certain physiopathology that drives to favored sites for metastasis, advanced ovarian cancers metastasize only to peritoneum while distant blood-borne metastases are reasonably infrequent (Cheng et al., 2009) (Cormio et al.). The recurrences are also frequently sited in the abdominal cavity, suggesting the function of a residual niche inside the peritoneum (Touboul et al., 2014).

If it is true that MSCs are able to modify the behavior of OCCs, is always true that the alterations strongly depend on the OCCs type.

For example, it was noticed that BM-MSCs are able to modify the mRNAs profile of two cell lines (Skov3 and Ovcar3) and that this remodeling is absolutely cell line dependent. Ovcar3 significantly upregulated 26 genes and downregulated 10 genes, while Skov3 displayed increased levels of 18 genes and decreased levels of 3 genes. These transcriptional modifications in the two ovarian cell lines are distinct and do not share a common gene signature. Nevertheless, through Ingenuity Pathway Analysis (IPA) software, it was possible to identify three common biological function clusters improved by the crosstalk with BM-MSCs, which are metastasis, proliferation and cell death of tumor cell line. The authors also determined that MSCs are able to promote cell proliferation and resistance to chemotherapy (Lis et al., 2012).

Moreover, as mentioned previously, it is important to remember that MSCs are different depending on the origin and on the stimuli that they receive.

In fact, as soon as they engraft in ovarian tumor microenvironment, cancer-associated MSCs exhibit an expression profile different from bone marrow MSCs. This expression profile display an augmented level of BMP-2, BMP-4 and BMP-6, and a significant decrease in PDGFRβ and TBX5 levels (McLean et al., 2011). de Lourdes showed in a recent work that Cervical Cancer derived MSCs (CeCa-MSCs) possess a greater capacity to suppress the proliferation, activation and effector functions of cytotoxic T-cells, and then to suppress the

anti tumor immune response, when compared to MSCs derived from normal cervical tissue (de Lourdes Mora-García et al., 2016).

In regards to this, a study conducted in the laboratory in which I carried out my PhD project, showed that exist several differences between HG-SOC-derived MSCs (HG-SOC-MSCs) and MSCs isolated from normal human adult tissues - among which bone marrow, heart, and adipose tissues – (N-MSCs) (Verardo et al., 2014).

***In vitro* growth potential**. First of all, even though they exhibit a similar mesenchymal morphology at the same population doubling level (PDL), the *in vitro* growth kinetics of HG-SOC-MSCs was higher when compared to the N-MSCs growth potential. In fact, the cell PDL were 30 ± 3 and 46 ± 15 hours for the HG-SOC-MSCs and the N-MSCs, respectively.

Surface immunophenotype. Both HG-SOC-MSCs and N-MSCs cell types showed a typical MSC-like cell surface marker profile (CD73, CD90), only CD105 was a marker less expressed in HG-SOC-MSCs; both the cell lines were positive for CD59, CD13, and CD49b, but negative for CD34 and CD45, which are hematopoietic system markers. Moreover, HG-SOC-MSCs unveiled a different pattern of surface adhesion molecules when compared to N-MSCs with a decreased level of FN binding integrins CD29, CD49a, and CD49d and a greater level of CD146/MCAM.

Biological functions and transcriptional regulators. N-MSCs and HG-SOC-MSCs have in common the triggering of shared core of biological functions and transcriptional regulators, the differences reside in the diverse grade of their activation.

Transcription signature and tissue specificity. Taking advantage of tools such as deep-CAGE and FANTOM5, it was discovered a cell-type-specific transcriptional activity and tissue specificity, which identifies HG-SOC-MSCs with respect to N-MSCs from other tissue districts and positions them close to primary mesothelial and mesothelial-derived cells. The figure 6 shows in the upper graph (fig. 6 A) a set of differentially expressed genes between HG-SOC-MSCs and N-MSCs, while in the lower graph (fig. 6 B) it is shown the mesothelial-related gene signature.

Clinical outcome. High levels of the aforementioned mesothelial-related gene signature (fig. 6 B) in patients correlates with a bad prognosis.

Interestingly, HG-SOC-MSCs do not show any chromosomic aberrations and result to be normal at a genomic level.

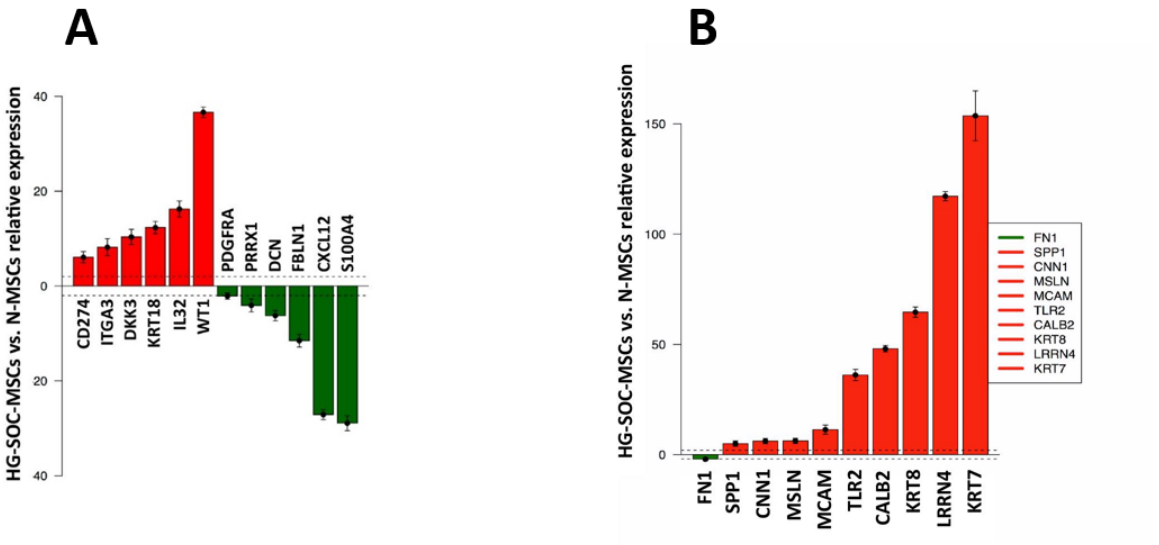

Figure 6 (Verardo et al., 2014).A) RT-qPCR validation of selected genes differentially expressed between HG-SOC-MSCs and N-MSCs. B) RT-qPCR validation of HG-SOC-MSCs mesothelial marker genes and selected mesothelial-related genes. Relative expression levels in HG-SOC-MSCs with respect to N-MSCs. All the genes are significantly over-expressed (at least $p < 0.05$) in HG-SOC-MSCs with respect to N-MSCs

2. Aim of the thesis

The starting point of this thesis was the transcriptome characterization of MSCs derived from High-Grade Serous Ovarian Cancer (HG-SOC-MSCs), performed at LNCIB by integrating data sets from a comprehensive collection of other normal MSCs (N-MSCs), normal and cancerous primary cells and tissues. This integrative analysis highlighted a mesothelial-specific signature of HG-SOC-MSCs pointing to the contribution of the mesothelial-derived environment within the tumor-supporting compartment. High-grade serous ovarian carcinoma (HG-SOC) possesses a great dissemination ability having direct access to a highly receptive environment, the mesothelial layer of the peritoneum. The dissemination involves the acquisition of specific phenotypes that allow carcinoma cells to exfoliate from the primary site into the peritoneal cavity, to attach to and communicate with the superficial layer of the mesothelium in the peritoneal cavity. It is proposed that the contribution of the hosting environment, including all the accessory stromal cells and mesothelium, is critical for the highly disseminative ability of HG-SOC. In order to address the mechanistic impact of HG-SOC-MSCs and have insights into their biological effects on the cancer cell compartment, we planned to setup two heterogeneous cell culture systems, in which an ovarian cancer-derived cell line (Skov3 stably expressing RFP) was co-cultured with MSCs (N-MSCs or HG-SOC-MSCs stably expressing GFP), thus mimicking the tumor-stroma interaction. We decided to setup both a simplified two-dimensional (2D) short-term (1 hour) co-culture system and a long-term (5 days) co-culture system. We wanted to gain insights into the transcriptional remodeling of Skov3 cells upon co-culture with HG-SOC-MSCs and into the functional impacts that this interaction could exert. We also planned to investigate whether injection of Skov3 cells co-cultured with HG-SOC-MSCs affects tumor appearance in a xenograft model. Since WT1 is one of the most differentially expressed genes identified in the previous HG-SOC-MSCs vs. N-MSCs comparative analysis, and a recognized global regulator of both stromal and endothelial tumor microenvironment, we decided to test its

possible involvement in the crosstalk between the two cell types used in the heterogeneous short-term co-culture system.

3. Material and Methods

Human samples

Human samples were obtained from the Azienda Ospedaliero Universitaria of Udine (AOU) and collected after informed consent in accordance with the declaration of Helsinki and with approval by Bioethics Committee. The records of the samples are reported in the following table (table1).

MSC line	Sex	Age	Tissue
HSLIM-15	F	35	Adipose
HSLIM-29	F	37	Adipose
HSLIM-45	F	61	Adipose
HSLIM-94	M	60	Adipose
HSLIM-118	F	74	Adipose
SOC-57-02	F	63	Serous Ovarian Carcinoma – Right ovary
SOC-60N	F	65	Serous Ovarian Carcinoma – Left and right ovaries
SOC-69N	F	73	Serous Ovarian Carcinoma - Left and right ovaries

Table 1

Isolation and *in vitro* expansion of HG-SOC-MSCs

Primary serous ovarian cancer samples were obtained from the Azienda Ospedaliero Universitaria (AOU) in accordance with consent procedures of the Bio-Ethic Committee. Surgical biopsies were freshly collected from patients undergoing surgery, washed several times in PBS solution and then mechanically disaggregated by mincing it with razor blades. Further disassociations were carried out by enzymatic digestion (20 µg/ml collagenase IV (StemCell Technologies)) for ten minutes at 37 °C. Single cell suspensions were obtained by filtering the disaggregated tissue through a nylon mesh with 70 µm pores (Cell Strainer, BD

falcon). Recovered cells were cultured in MyeloCult Medium (StemCell Technologies) containing 25% of serum (12.5 % horse serum and 12.5 % of fetal bovine serum (both StemCell Technologies)). After colony formation, the cells were detached with 0.25% trypsin-EDTA (Sigma-Aldrich) and re-plated at a density of $2.5x10^3/cm^2$ onto fibronectin (Sigma-Aldrich) coated 100 mm dishes (Sacco-Falcon) in a expansion medium composed as follows: 60% low glucose DMEM (Invitrogen), 40% MCDB-201, 1 mg/mL linoleic acid-BSA, 10^{-9} M dexamethasone, 10^{-4} M ascorbic acid-2 phosphate, 1X insulin-transferrin-sodium selenite (all from Sigma-Aldrich), 2.5 % fetal bovine serum (StemCell Technologies), 10 ng/mL hPDGF-BB, 10 ng/mL hEGF (both from Peprotech EC). Fresh medium was replaced every 3-4 days.

Retroviral Infection

To obtain Skov3 stably expressing RFP and MSCs stably expressing GFP, HEK293GP were seeded in a 10 cm Petri dish (Sacco-Falcon) at a final concentration of 1.5×10^6 and were transfected after 24 hours with 7.5 µg of retroviral vector (pLPC-DsRed2 and pLCP-eGFP respectively) (Serrano et al., 1997) and 7.5 µg of env vector pMD2 (https://www.addgene.org/12259/). 24 hours after the transfection, the medium was refreshed. Then, after 48 hours, the supernatant was collected and filtered with 0.45 µm filter (EuroClone) and was enriched with 1 mL of fetal bovine serum and 800 ug/mL polybrene. The supernatant was used to infect the respective target cells (Skov3 and MSCs) and the puromycin selection (5 µg/mL) was applied the day after.

Short-term (1 hour) co-culture

2.5 x 10^5 Skov3 RFP cells were plated as control and 5 x 10^5 mesenchymal stromal cells stably expressing GFP, both cancer-derived and normal, were seeded in a mesenchymal-specific expansion medium (the composition is described above) into a fibronectin (Sigma-Aldrich)-coated 100 mm Petri dish (Sacco-Falcon) and incubated in 5% CO_2 and 5 % O_2 incubator for 3 days in order to reach 70% confluence. After 48 hours from the seeding, the medium was refreshed and 24 hours later the medium was filtered with 0.45 µm filter (EuroClone) in order to get rid of all the dead cells. Then, 7.5 x 10^5 Skov3 RFP were plated on the respective layers, or the media were filtered in fresh new 100 mm Petri dishes (Sacco-Falcon) and Skov3 RFP cells were plated in the Skov3 RFP- and HG-SOC-MSCs-derived conditioned media, for 1 hour. A mechanical shaking approach was used to minimize the attachment of ovarian cancer cells on the respective layers. After 1 hour of co-culture Skov3 RFP cells were isolated, sorted by FACS sorter BD FACSAria II and plated for the experiments or treated to isolate RNA. Skov3 RFP were plated in DMEM 4.5 g/l glucose with 10% fetal bovine serum and 1% penicillin/streptomycin (100 U/mL Penicillin and 100 U/mL Streptomycin) (Lonza).

WT1 silencing in HG-SOC-MSCs-eGFP

A total of 5 x 10^5 HG-SOC-MSCs eGFP were seeded into fibronectin-coated 100 mm Petri dish (Sacco-Falcon) and simultaneously transfected with siRNA targeting WT1 (Eurofins genomics) at a final concentration of 24 nM using Lipofectamine™ RNAiMAX Transfection Reagent according to the manufacturer's specifications (ThermoFisher Scientific). A scrambled siRNA control (siControl) was purchased from QIAGEN. All procedures were performed in an RNase-free environment to minimize the cytotoxicity of the reagent itself, cells were plated into a medium without antibiotics and the medium was refreshed after 6-8

hours. Cells were either harvested for RNA extraction 72 hours after transfection, or used as a layer to perform short-term co-culture.

SiWT1 sequence	5'-AUGAAUUAGUCCGCCAUCACATT-3'

Three siRNAs have been tested and the selected one was the only with a high silencing efficiency. Moreover, the mentioned siRNA targets specifically 3 WT1 isoforms: A (-KTS), B (-KTS) and D (+KTS), respectively (Bissanum et al., 2017). It is known that, even though WT1 (+KTS) and WT1 (−KTS) isoform functions are partially redundant, WT1(−KTS) has a role mainly as transcriptional regulator, while WT1(+KTS) acts in the RNA processing (Dutton et al., 2006). Nevertheless, since only one siRNA has been used in this thesis, we cannot exclude off-targets.

Long-term (5 days) co-culture

$3x10^5$ Skov3 RFP and MSCs eGFP (both HG-SOC- and N-MSCs) were plated as control in 100 mm Petri dish (Sacco-Falcon) while an admix of Skov3 RFP and MSCs eGFP was plated at a final concentration of $6x10^5$/100 mm Petri dish with a ratio of 1:3 respectively. Cells were cultured for 5 days in the mesenchymal-specific expansion medium described above and then sorted by taking advantage of FACS sorting technology.

Long-term (5 days) membrane-separated co-culture

HG-SOC-MSCs eGFP were plated in a 6 well plate (EuroClone) at a concentration of $4.5x10^4$ cells in 3ml of MSC specific expansion medium, while Skov3 RFP were plated in the cell culture insert above (BD Falcon 0.4um pore size) the HG-SOC-MSC layers ($1.5x10^4$ Skov3 RFP in 2ml of MSC specific-medium)

The same cell numbers were used for the controls. HG-SOC-MSC were plated in a 6 well plate (3ml of MSC-medium) and the insert above was filled with 2 mL of medium but no Skov3 RFP; while the Skov3 RFP were plated in the insert with 2 mL of MSC medium above a layer of $1.5x10^4$ Skov3 RFP seeded in 3 mL of MSCs medium.

FACS Sorting

Upon short-term co-culture, Skov3 RFP cells were collected in PBS/EDTA 5 mM and sorted taking advantage of BD FACSAria II sorter with a 100 µm noozle. The dsRED signal was collected through a 582/15 bandpass filter (PE, DsRed). A light scatter gate was drawn in the SSC versus FS plot to exclude debris and include the viable cells. Cells in the gate were displayed in a single-parameter histogram for the dsRED and final gating settings determined to collect the labeled cells. Post-sorting, the cells were collected in DMEM 4.5 g/l glucose with 10 % fetal bovine serum and 1% penicillin/streptomycin (100 U/mL Penicillin and 100 U/mL Streptomycin) (Lonza) and used according to the planned experiment.

Upon long-term co-culture, Skov3 RFP, MSCs eGFP as controls and Skov3 RFP/MSCs eGFP admix were collected in PBS/EDTA 5 mM and sorted taking advantage of BD FACSAria III sorter. The dsRED signal was collected through a 582/15 bandpass filter (PE, DsRed), while the eGFP signal was collected through a 530/30 bandpass filter (FITC). Cells in the gate were displayed in a single-parameter histogram for the dsRED and FITC respectively, and final gating settings determined to collect the labeled cells. Post-sorting, the cells were collected in QIAzol Lysis Reagent (QIAGEN).

Microarray data generation and analysis

Total RNA was extracted using the RNeasy Mini Kit (Qiagen), according to the manufacturer's protocol. Synthesis of cDNA and biotinylated cRNA (from 500 ng total RNA) was performed using the Illumina TotalPrep RNA Amplification Kit (Ambion),

according to the manufacturer's protocol. Quality assessment and quantitation of total RNA and cRNAs were performed with Agilent RNA kits on a Bioanalyzer 2100 System (Agilent). Hybridization of cRNAs (750 ng) was carried out using Illumina Human 48K gene chips (Human HT-12 v4 Expression BeadChip). Array chip washing was performed in High Temp Wash Buffer (Illumina) at 55°C for 10 min, followed by staining using streptavidin-Cy3 dyes (Amersham Biosciences,). Hybridized arrays were stained and scanned in a BeadStation 500 System (Illumina). Data have been normalized with the cubic spline method (Workman et al., 2002) using Illumina BeadStudio. Differential genes expression analysis has been performed using the limma package (Ritchie et al., 2015). Genes with corrected p-value<0.1 were selected as differentially expressed (see below).

FANTOM5 data analysis

The robust transcriptional (RLE) activity peaks count FANTOM5 data matrices ((DGT) et al., 2014) were used for the differential transcriptional analysis of HG-SOC-MSCs and N-MSCs. EdgeR (Robinson et al., 2010) package for R/Bioconductor Environment (Gentleman et al., 2004) was used for statistical analysis as described in Verardo et al., 2014.

Functional and upstream regulation analysis

Starting from the list of differentially expressed genes we performed functional enrichment analysis (Huang et al., 2008) and gene set enrichment analysis (Subramanian et al., 2005).
Differentially expressed genes were further analyzed using Ingenuity Pathway Analysis (IPA, Ingenuity® Systems, www.ingenuity.com). We used an adjusted p-value of 0.1 because we wanted to generate comparable gene lists for both the analysis (co-cultures with HG-SOC-MSCs and with N-MSCs). We are actually generating other replicates for the co-cultures with N-MSCs in order to increase the statistical significance.

The approach we used for the functional analysis (IPA) takes into account the fold change and the significance in order to obtain quantification of activation/repression of functions, pathways and upstream regulators: in this way, also genes with low differential expression or low significance can be used as input and are informative. The prediction of the transcription factors and regulative molecules was obtained using the Upstream regulators function (IPA suite). For every upstream regulator an overlap p-value and a z-score are calculated: the p-value indicates the significance based on the overlap between dataset genes and known targets regulated by the molecule, while the z-score is used to infer the possible activation (z-score > 0) or inhibition (z-score < 0) of the molecule based on prior knowledge stored in the proprietary Ingenuity Knowledge Base.

Cellular compartment specific protein-protein interactions have been obtained from ComPPI database (Veres et al., 2015) selecting only membrane and extracellular validated interactions.

Mapping between entrez gene IDs and protein IDs have been performed using the Uniprot Retrive/ID mapping tool.

All statistical analysis and calculations have been performed in R statistical environment (https://www.R-project.org/).

RNA extraction

Total RNA was isolated from cell culture by using QIAzol Lysis Reagent (QIAGEN) according to the manufacturer's specifications. RNA concentration and its purity was quantified by using NanoDrop ND-1000 Spectrophotometer.

cDNA synthesis

cDNA was produced using the QuantiTect Reverse Transcription Kit (Qiagen).

In the genomic DNA elimination reaction: 1 µL of gDNA Wipeout Buffer, 0.5 µg of template RNA and RNAase-free water up to 7 µL were mixed together and incubated for 2 minutes at 42°C and placed on ice immediately after.

In the following reverse-transcription reaction: 0.5 µL of Quantiscript Reverse Transcriptase, 2 µL of Quantiscript RT buffer and 0.5 µL of RT Primer Mix were added to the genomic DNA elimination reaction for a total of 10 µL and incubated for 30 minutes at 42°C and for 3 minutes at 95°C .

Real-Time Quantitative RT-qPCR

Real-time quantitative RT-qPCR was performed using the SYBR Green Master Mix (Applied Biosystems, Life Technologies, Carlsbad, CA) on a StepOnePlus Real-Time System (Applied Biosystems). Thermocycle conditions included initial denaturation at 95°C (10 min each), followed by 40 cycles at 95°C (15 s) and 60°C (1 min). The expression level of each target gene was normalized to beta-actin (ACTB).

GENE ID	FORWARD PRIMER (5'-3')	REVERSE PRIMER (5'-3')
ACTB	CCAACCGCGAGAAGATGA	CCAGAGGCGTACAGGGATAG
ALDH1A3	CTCTTCATCAAACCCACTGT	TCACCTAGTTCTCTGCCATT
ATF4	GTTCTCCAGCGACAAGGCTA	ATCCTGCTTGCTGTTGTTGG
CTGF	CGACTGGAAGACACGTTTGG	AGGCTTGGAGATTTTGGGAG
CXCL1	TTGCCTCAATCCTGCATCCC	TTGGATTTGTCACTGTTCAGCA
CXCL2	TGCCAGTGCTTGCAGAC	TCTTAACCATGGGCGATGC
CYR61	AGCCTCGCATCCTATACAACC	TTCTTTCACAA GGCGGCACTC
EGR1	CTTCAACCCTCAGGCGGACA	GGAAAAGCGGCCAGTATAGGT
FOS	CCCTGCAGTCCGGATACTCA	TCACGTCCCACGACCTTGA
IL1β	GCCTGAAGCCCTTGCTGTAGT	GCGGCATCCAGCTACGAA
IL8	GGCAGCCTTCCTGATTTCTG	CTTGGCAAAACTGCACCTTCA
LRRN4	TTCCTCAGGTAGAGGGATGTGAGCTT	TGGTCACGCTCGAAGTCCTGGAT
MT1E	AGCATCCCCTTTGCTCGAAAT	CAGCTGCACTTCTCCGATG
PDPN	CCAGGAACCAGCGAAGACC	GCGTGGACTGTGCTTTCTGA
SOCS3	TCCCCCCAGAAGAGCCTATTAC	TCCGACAGAGATGCTGAAGAGTG
TNF	TAGGCTGTTCCCATGTAGCC	CAGAGGCTCAGCAATGAGTG
WT1	ACTCTTGTACGGTCGGCATC	TGAGCTGGTCTGAACGAGAA

Table 2

Wst-1 assay.

Upon short-term co-culture on different layers, Skov3 RFP cells were sorted, collected and plated in 96 wells plate (EuroClone) at different concentrations for 12, 36 and 72 hours. Skov3 RFP cells were then incubated for 30 minutes with Cell Proliferation Reagent WST-1 (Roche) at the final concentration of 0.1%. The absorbance of the product (wavelength: 440 nm) was read with EnSpire Multimode Plate Reader (PerkinElmer).

Automatic cell counting.

Upon short-term co-culture on different layers, Skov3 RFP cells were sorted, collected and plated in 96 wells plate (ViewPlate-96 F TC, PerkinElmer) at different concentration for 12, 36 and 72 hours. Cells were washed twice with PBS, fixed with 3% PFA and nuclei were stained with Hoescht dye. The number of cells was then quantified by using a multimode plate reading machine (PerkinElmer) able to take 16 random pictures/well and to quantify the number of the blue objects (nuclei). All the data were analyzed by using MetaXpress High-Content Image Acquisition and Analysis Software.

Growth in low attachment (Gila) assay.

Upon short-term co-culture on different layers, Skov3 RFP cells were sorted, collected and plated into ultralow-attachment surface 96 wells plates (Corning) at a concentration of $9x10^3$ cells/well. After five days from the seeding, cells aggregates were incubated for 4 hours with Cell Proliferation Reagent WST-1 (Roche) at the final concentration of 0.1%. Vitality of cells aggregates was then assayed for WST1 content, taking advantage of EnSpire Multimode Plate Reader (PerkinElmer).

Transwell assay

Upon short-term co-culture, $2x10^5$ Skov3 RFP were plated in serum-free medium in a 8.0 µm cell culture insert (Falcon) located in 24 well plates (Falcon). At the bottom of each well, 500 uL of medium enriched with 10% fetal bovine serum was added to encourage the migration. After 16 hours, cells that migrated through the insert towards the enriched medium were fixed with 3% PFA, dyed with 0.1 % crystal violet and counted at the optical microscope with 20X of magnificence.

In vivo subcutaneously injection of Skov3 RFP and HG-SOC-MSCs eGFP admix into SCID mice

$2x10^5$ Skov3 RFP cells (n=15) alone or $2x10^5$ Skov3 RFP cells admixed with $2x10^5$ HG-SOC-MSCs eGFP (n=16) were subcutaneously injected into NOD SCID mice. Once a primary tumor was detected, its growth was monitored, and the animal was sacrificed when the tumor had reached 1cm in diameter (as evaluated by the caliper). As control, also HG-SOC-MSCs eGFP alone were injected into NOD SCID mice with a concentration from $2x10^5$ to $4x10^5$ cells/mouse.

4. Results

4.1 A new technical approach to study short-term co-culture.

In the lab in which I carried out my PhD project, it was developed a new 2D simplified system to study short-term co-cultures. Indeed, this technique consists of a transient contact between MSCs eGFP (both cancer-derived and normal) and Skov3 RFP for one hour, as widely explained in the material and methods chapter.

We noticed that Skov3 RFP cells maintained in suspension tend to adhere to the below attached layer of cells with different affinity, depending on the attached cell type. In fact, they adhere with more affinity to the HG-SOC-MSCs eGFP layer than to the Skov3 homo-layer or the N-MSCs eGFP layer. We performed the short-term co-culture experiments in 100 mm cell-culture dishes. Using N-MSCs eGFP or Skov3 RFP cells as the attached cell layers and co-culturing 7.5 x 10^5 Skov3 RFP cells for 1 hour under gentle mechanical shaking, we normally collected 2 x 10^5 cancerous cells. Instead, when using HG-SOC-MSCs eGFP as the attached cell layer, the number of the collected Skov3 RFP cells dropped to 1.0-1.5 x 10^5. We also wanted to test whether among the collected cells there was a fraction of cells detached from the below layer. Using an automated cell counter and relying on the RFP and eGFP labels of the two cell types (Skov3 RFP, HG-SOC-MSCs eGFP) we were able to show that a 3% fraction of HG-SOC-MSCs was present among the collected cells. For this reason, in order to get rid of the contaminating fraction of the detached cells, FACS sorting was applied on the collected cells. After titration experiments, 1 hour was established to be the maximum experimental time point, since for longer times Skov3 RFP cells were irreversibly attached to the below cell layers making it impossible to collect a proper number of cells. After the short-term co-culture experiments, Skov3 RFP cells were then collected, sorted and used for the subsequent experiments.

In this thesis, we are considering the hypothesis that Skov3 phenotype is inducted by HG-SOC-MSCs following short term co-culture, but, since Skov3 cells adhere to the HG-SOC-MSCs layer with a greater affinity when compared to N-MSCs layer, it is also possible that

the mentioned phenotype derives from a Skov3 selection carried by HG-SOC-MSCs. Thus, Skov3 cells attached to the HG-SOC-MSCs layers could be phenotypically different from the not attached. This point is further explained in the Future Perspective chapter.

4.2 Short-term co-culture with HG-SOC-MSCs eGFP specifically remodels the transcriptional activity of Skov3 RFP cells.

Taking advantage of Illumina technology, microarray analysis was performed on sorted Skov3 RFP cells upon short-term co-culture with MSCs. A cluster of genes differentially upregulated in Skov3 RFP cells upon transient contact with HG-SOC-MSCs eGFP and not with N-MSCs eGFP was identified. Among the identified candidates, four genes (ALDH1A3, IL1β, PDPN and MT1E) were validated by RT-qPCR. MT1E expression was also found to be upregulated after the co-culture with N-MSCs eGFP, even though at a considerably lower level when compared to the co-culture with HG-SOC-MSCs eGFP. Interestingly, when Skov3 RFP cells were cultured for 1 hour in HG-SOC-MSCs eGFP conditioned medium (figure 7), the expression of the four selected genes in Skov3 RFP cells was comparable to that observed when cultured in the control medium (Skov3 RFP conditioned medium). Remarkably, all the mentioned genes are involved in tumor progression. ALDH1A3 (Aldehyde Dehydrogenase 1 Family Member A3) is a member of the super family of enzymes ALDH and it is involved in the retinoic acid pathway (Rodriguez-Torres and Allan, 2016). It strongly contributes to tumor cells growth, migration, invasion and thus to metastatic behavior (Marcato et al., 2015). IL-1β (Interleukin-1β) is a cytokine that stimulates tumorigenesis by mediating inflammatory response (Schauer et al., 2013) Interestingly, IL-1β appears also to have a role in ovarian cancer metastasis, facilitating the dissemination in the peritoneum (Watanabe et al., 2012). PDPN (Podoplanin) is a 38–44 kDa O-glycosylated transmembrane glycoprotein. PDPN-expressing cancer cells have enhanced malignant potential which promotes metastasis (Kunita et al., 2011), alteration of

cell morphology and motility (Scholl et al., 1999) (Wicki et al., 2006), and epithelial-mesenchymal transition (Martin-Villar et al., 2006). MT1E (Metallothionein1E) is a low-molecular weight intracellular metalloprotein and it is shown to be essential for tumor migration (Wu et al., 2008).

.

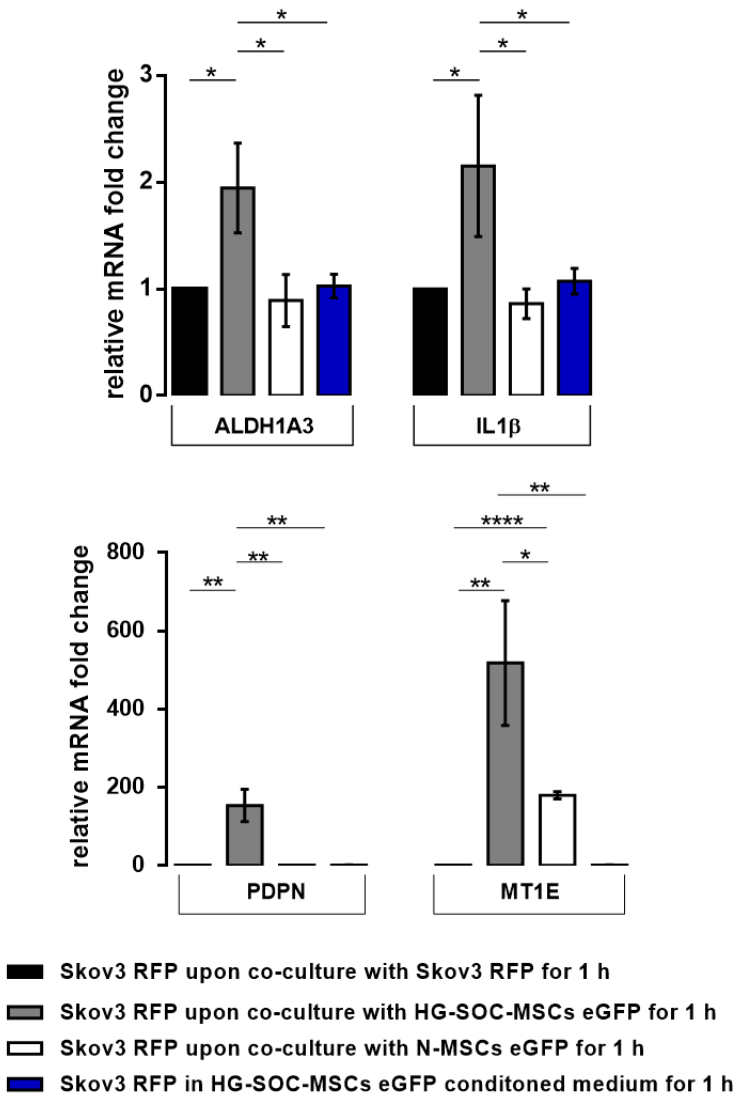

Figure 7.Short-term co-culture with HG-SOC-MSCs eGFP induced an increased expression of ALDH1A3, IL1β, PDPN and MT1E in Skov3 RFP with respect to N-MSCs eGFP or HG-SOC-MSCs eGFP conditioned medium. Skov3 RFP in Skov3 RFP conditioned medium was used as control for the conditioned medium experiments, but was not reported in the graph for stylistic reasons.

4.3 Direct short-term co-culture with HG-SOC-MSCs eGFP specifically increases Skov3 RFP viability

After short-term co-culture with HG-SOC-MSCs eGFP, Skov3 RFP cells were sorted and equal numbers of cells were seeded on proper 96 well-plates and observed after different time points (12, 36 and 72 hours). As can be seen if Fig.8B the number of cells attached at 36 hrs after seeding is visibly higher for Skov3 RFP previously short-term co-cultured with HG-SOC-MSCs eGFP with respect to the other co-culture controls and such difference remains constant in the following time points. In the same experimental settings, BrdU incorporation assays gave no significant difference (data not shown) pointing to an increased proliferation-independent viability (fig 8B vs A) for the short-term contact with HG-SOC-MSCs. Interestingly, it was noticed that the Skov3 RFP isolated and plated upon co-culture with HG-SOC-MSCs displayed an improved capacity to attach to the well-plate surface, when compared to the other co-culture settings or conditioned media experiments.

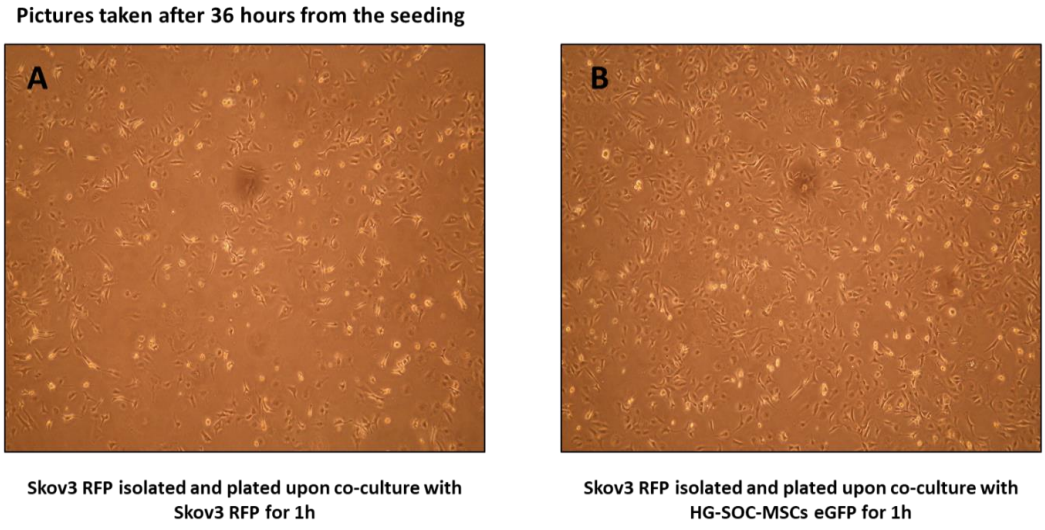

Figure 8. On the left (A), Skov3 RFP after 36 hours from the seeding upon short-term co-culture with Skov3 RFP layer. On the right (B), Skov3 RFP after 36 hours from the seeding upon short-term co-culture with HG-SOC-MSCs eGFP layer. The pictures show that Skov3 RFP cells displayed a higher viability in consequence to the influence of the HG-SOC-MSCs eGFP.

Given this observation, we decided to perform automated cell count and WST1 assay at 12, 36 and 72 hours on Skov3 RFP sorted and seeded after the short-term co-culture experiments (taking into consideration that the population doubling time of Skov3 RFP is 36 hours). Interestingly, Skov3 RFP cells viability was strongly affected by the direct short- term co-culture with HG-SOC-MSCs eGFP, but not (or at a significantly lower level) with N-MSCs eGFP or by the culture in the HG-SOC-MSCs eGFP conditioned medium for 1 hour (figure 9).

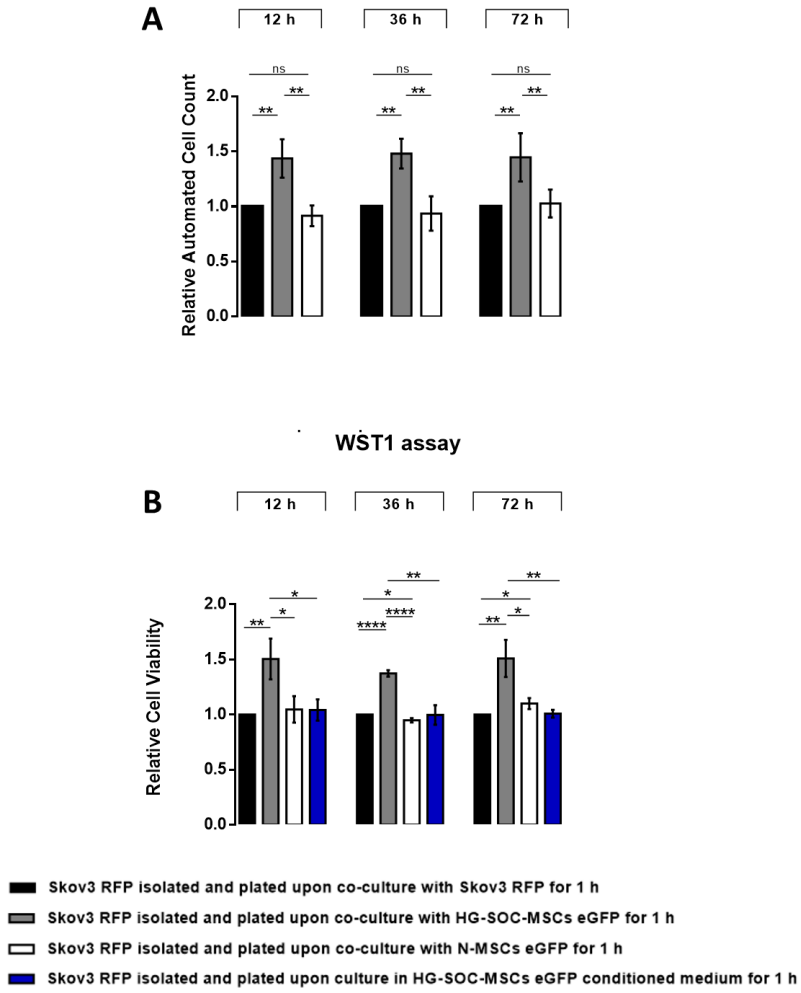

Figure 9. A) Relative automated cells count of Skov3 RFP isolated and plated upon short-term co-culture with Skov3 RFP (black bars), with HG-SOC-MSCs eGFP (grey bars) and with N-MSCs eGFP (white bars), showed increased cell numbers at different time points (12, 36, 72 hours) specifically after 1 hour of co-culture with HG-SOC-MSCs eGFP. B) Viability assay of Skov3 RFP isolated and seeded upon

short-term co-culture with Skov3 RFP (black bars), with HG-SOC-MSCs eGFP (grey bars), with N-MSCs eGFP (white bars) and cultured in HG-SOC-MSCs eGFP conditioned medium (blue bars), showed an augmented viability at different time points (12, 36, 72 hours) after 1 hour of transient direct co-culture with HG-SOC-MSCs eGFP only.

4.4 Skov3 RFP cells increase their motility following short-term co-culture with HG-SOC-MSCs eGFP.

As already mentioned, the genes upregulated following short-term co-culture with HG-SOC-MSCs eGFP are related to the migration process. For this reason, we decided to investigate if, in the model we studied, Skov3 RFP motility could be influenced by short-term co-culture with HG-SOC-MSCs.

Surprisingly, we showed that the 1-hour transient co-culture with HG-SOC-MSCs eGFP was able to induce a significantly greater motility in Skov3 RFP cells and that the transient contact between the two cell populations was necessary to obtain this result. In fact, this effect cannot be observed if Skov3 RFP cells are cultured for 1 hour in HG-SOC-MSCs eGFP conditioned medium.

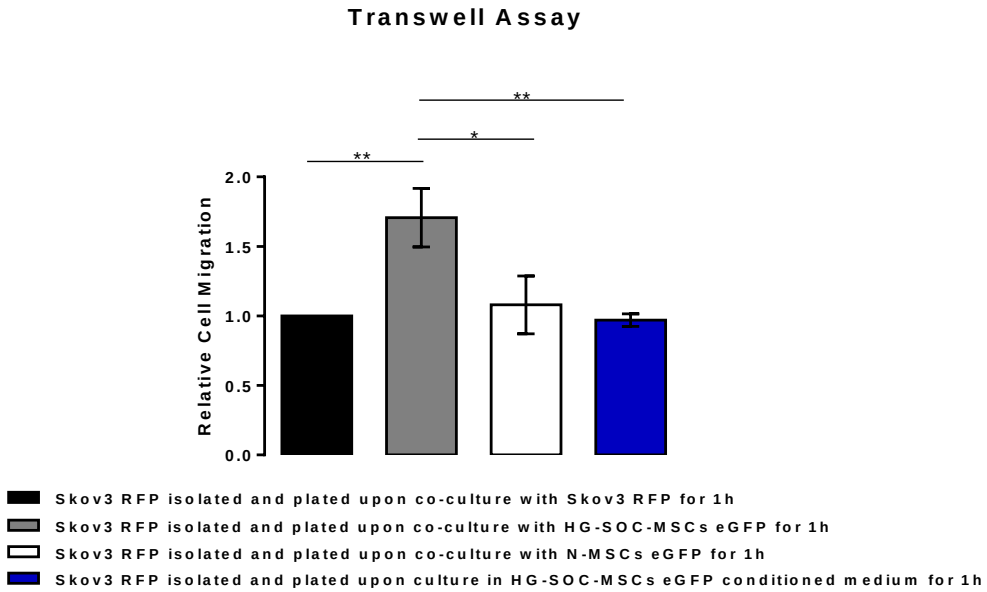

Figure 10. Transwell assay showed that short-term co-culture with HG-SOC-MSCs eGFP (grey bars) specifically increased the motility of Skov3 RFP when related to the co-culture with the control layer (black bars), the N-MSCs eGFP (white bars) or the culture in HG-SOC-MSCs eGFP conditioned medium for 1 hour (blue bars).

4.5 Skov3 RFP cells exhibit an increased anchorage-indipendent growth following short-term co-culture with HG-SOC-MSCs eGFP.

All the reported data pointed to the enhancement of the neoplastic properties of Skov3 RFP upon short-term co-culture with HG-SOC-MSCs eGFP. We decided to investigate whether the short-term co-culture was able to modulate the tumorigenic potential, taking advantage of the GILA assay.

In fact, the GILA assay is based on the ability of transformed cells to grow on low-attachment plates, on the contrary of not transformed cells. It is comparable to the soft agar assay for the measure of tumorigenicity/transformation of cells, with the advantage that it is faster and can be used for high-throughput analysis (Rotem et al., 2015).

Remarkably, sorted Skov3 RFP cells, upon transient direct short-term co-culture with HG-SOC-MSCs eGFP, displayed an increased tumorigenicity, in terms of viability of cells aggregates, when related to co-culture with N-MSCs eGFP or to culture in HG-SOC-MSCs eGFP conditioned medium for 1 hour (fig. 11).

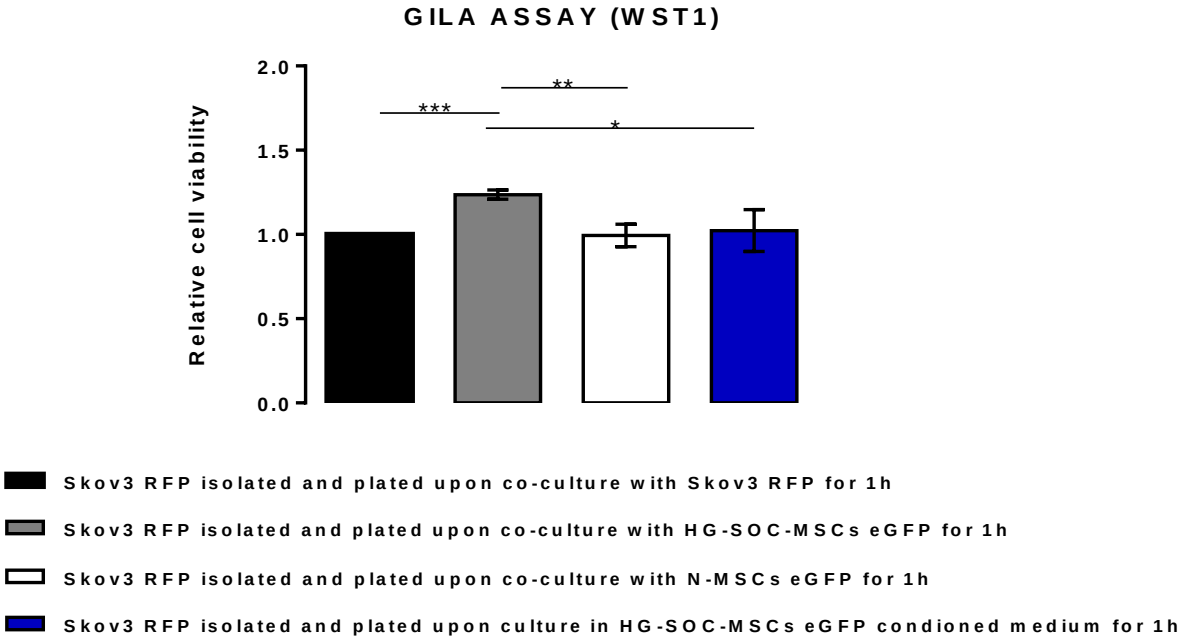

Figure 11. WST1 assay showed that Skov3 RFP upon short-term co-culture with HG-SOC-MSCs eGFP (grey bars) displayed a significant higher percentage of viable cell aggregates when compared to co-culture with N-MSCs eGFP (white bars) or to culture in HG-SOC-MSCs eGFP conditioned medium (blue bars).

4.6 Long-term co-culture with HG-SOC-MSCs eGFP transcriptionally remodel Skov3 RFP

Gene expression profile analysis by DNA microarrays was performed on Skov3 RFP cells following 5 days co-culture with both HG-SOC-MSCs eGFP (fig.12) and N-MSCs eGFP. We were able to identify 81 genes differentially expressed after HG-SOC-MSCs co-culture (table 1 in Supplementary; adj.p.value <0.1 (see material and methods)) and, among them, some of the most upregulated (IL8, IL6, CXCL1, CXCL2) are pro-inflammatory cytokines responsible not only for inflammatory response, but also for chemoattraction, proliferation and recruitment of leukocytes. We took advantage of Ingenuity Pathway Analysis (*IPA*) functional analysis tool to directly compare the transcriptional program of Skov3 RFP co-cultured with HG-SOC-MSCs eGFP and N-MSCs eGFP. The analysis takes into account the entire transcriptional program of the two conditions and compares the activation of specific pathways and functions: this approach permits to compare at a quantitative level the predicted functional relevance of the two transcriptional programs. A quantitative approach, in alternative to a classical enrichment approach, is desirable in our contest since we already know that in HG-SOC-MSCs and N-MSCs the same pathways and functions are activated but at different levels (Verardo et al., 2014). Functional analysis performed on the generated expression data allowed us to highlight the activation of several functional themes.

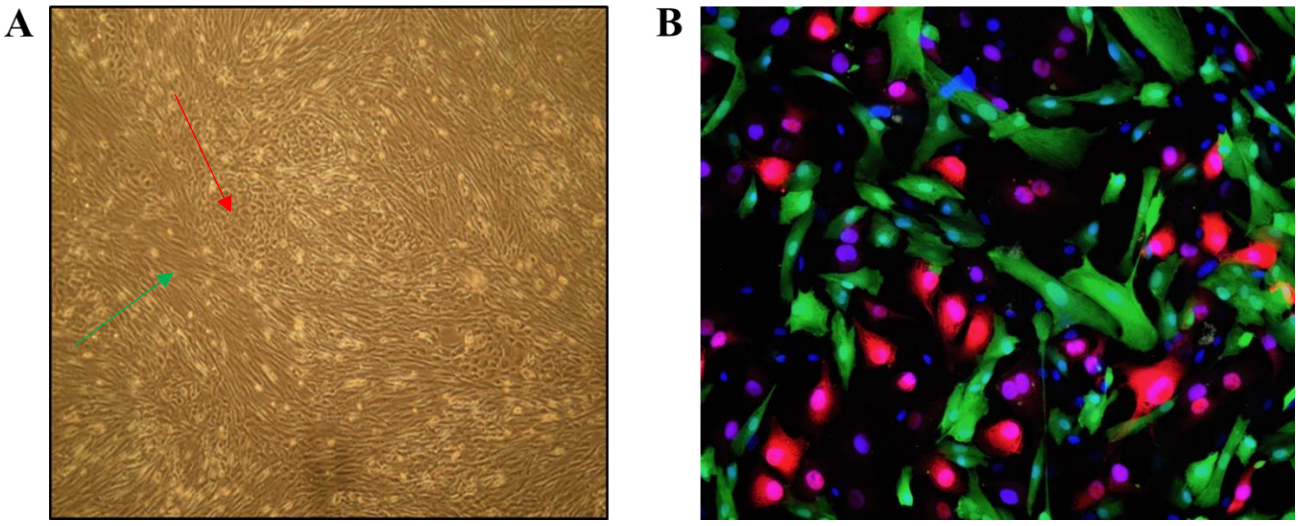

Figure 12.A. Representative picture of 5 days co-culture of HG-SOC-MSCs eGFP (green arrow) and Skov3 RFP (red arrow) taken at the optical microscope. B. Representative picture of 5 days co-culture of HG-SOC-MSCs eGFP (in green) and Skov3 RFP (in red). Nuclei are stained with hoechst (blue).

The functional analysis, allowed us to highlight the activation of several functional themes in HG-SOC-MSCs co-cultures respect to N-MSCs co-cultures: some important cancer-related processes such as “Adhesion of tumor cell lines”, ”Development of connective tissue cells”, “Chemo attraction” and pathways such as “Acute Phase Response Signaling”, “Death Receptor Signaling” and “IL-8 Signaling” were identified (table 3 and table 4, respectively) and were sensibly more activated in Skov3 co-cultured with HG-SOC-MSCs.(Complete tables are available in Supplementary section, table 2 and 3 respectively)

Classical enrichment analysis (performed using David/Ease and GSEA, table 4 and 5 respectively in Supplementary) gave us similar results revealing an enrichment for TNF signaling pathway ($p=2^{-10}$), inflammatory response ($p=2^{-7}$), TNF signaling via NFKB ($p=6.7^{-45}$) and hypoxia ($p=7.7^{-23}$) in Skov3 co-cultured with HG-SOC-MSCs respect to control.

Biological term up-regulated in co-cultured Skov3 RFP	Delta z-score	Biological term down-regulated in co-cultured Skov3 RFP	Delta z-score
Adhesion of immune cells	3,30	Degradation of connective tissue	-0,78
Adhesion of tumor cell lines	3,21	Apoptosis of blood cells	-1,06
Development of connective tissue cells	2,89	Binding of mesothelial cells	-1,39
Chemoattraction	2,62	Differentiation of adipocytes	-1,47
Recruitment of myeloid cells	1,62	Growth Failure	-4,33

Table 3. Top functional themes up- and down- regulated in Skov3 RFP upon co-culture with HG-SOC-MSCs eGFP vs N-MSCs eGFP (positive values mean that functional themes are more activated in Skov3 RFP upon co-culture with HG-SOC-MSCs eGFP and negative values mean that functional themes are more activated in Skov3 RFP upon co-culture with N-MSCs eGFP). All functional themes are significantly enriched ($p<0.05$). Deltas of activation Z-scores are shown.

Pathways up-regulated in co-cultured Skov3 RFP	Delta z-score	Pathways down-regulated in co-cultured Skov3 RFP	Delta z-score
HMGB1 Signaling	1,87	Toll-like Receptor Signaling	-0,37
p38 MAPK Signaling	1,45	GNRH Signaling	-0,64
Acute Phase Response Signaling	0,87	HGF Signaling	-0,76
Death Receptor Signaling	0,60	Leukocyte Extravasation Signaling	-2,51
IL-8 Signaling	0,36	GP6 Signaling Pathway	-3,34

Table 4. Top pathways up- and down- regulated in Skov3 RFP upon co-culture with HG-SOC-MSCs eGFP vs N-MSCs eGFP (positive values mean that pathways are more activated in Skov3 RFP upon co-culture with HG-SOC-MSCs eGFP and negative values mean that pathways are more activated in Skov3 RFP upon co-culture with N-MSCs eGFP). All pathways are significantly enriched ($p<0.05$). Deltas of activation Z-scores are shown.

Moreover, we used the IPA to predict the upstream regulators that could possibly be the cause of the observed transcriptional program. In the table below (table 5), top upstream regulators are shown, the list with all the regulators is available in the supplementary (Supplementary.Table 6). Among these, for example, there are genes involved in ER stress signaling such as ATF4 and XBP1, in inflammation

pathways such as IFN-gamma, in cell migration and proliferation (SPARC) and cell growth and development (TGFB1). Moreover, some genes such as ABCA1 and TGFB1 appear also in the membrane protein-protein interaction prediction illustrated in the paragraph below.

Upstream regulators up-regulated in co-cultured Skov3 RFP	Delta z-score	Upstream regulators down-regulated in co-cultured Skov3 RFP	Delta z-score
ATF4	3,85	TGFB1	-1,35
IFNG	3,74	SPARC	-2,93
ALDH1A2	3,54	XBP1	-3,08
MYC	3,32	CD44	-3,86
ABCA1	2,33	SIRT2	-4,24

Table 5. Top upstream regulators up- and down- regulated in Skov3 RFP upon co-culture with HG-SOC-MSCs eGFP vs N-MSCs eGFP (positive values mean that genes are more expressed in Skov3 RFP upon co-culture with HG-SOC-MSCs eGFP and negative values mean that genes are more expressed in Skov3 RFP upon co-culture with N-MSCs eGFP). All regulators are significantly enriched ($p<0.05$). Deltas of activation Z-scores are shown.

4.7 Membrane protein-protein interaction prediction upon long-term co-culture.

The predicted regulators (table 6 in Supplementary) are not only transcription factors, but also membrane receptors and cytokines. Based on our previous results, we decided to focus our analysis on membrane and extracellular regulators. We calculated the delta of the activation z-score between Skov3 RFP upon co-cultures with HG-SOC-MSCs eGFP and N-MSCs eGFP for each selected regulator in order to quantify its specificity for the cancer- derived MSCs co-cultures. Then, we compared the activation Z-score delta of each regulator to the expression levels of the same genes in HG-SOC-MSCs and N-MSCs. Figure 13 shows activation Z-score deltas and expression logFC between HG-SOC-MSCs and N-MSCs (positive values mean that genes are more expressed in HG-SOC-MSCs). This data can explain part of the transcriptional program after co-cultures since membrane and extracellular regulators such as IL1-α, IL1-β, CXCL1 and other inflammation-related genes are actually more expressed in HG-SOC-MSCs respect to normal MSCs.

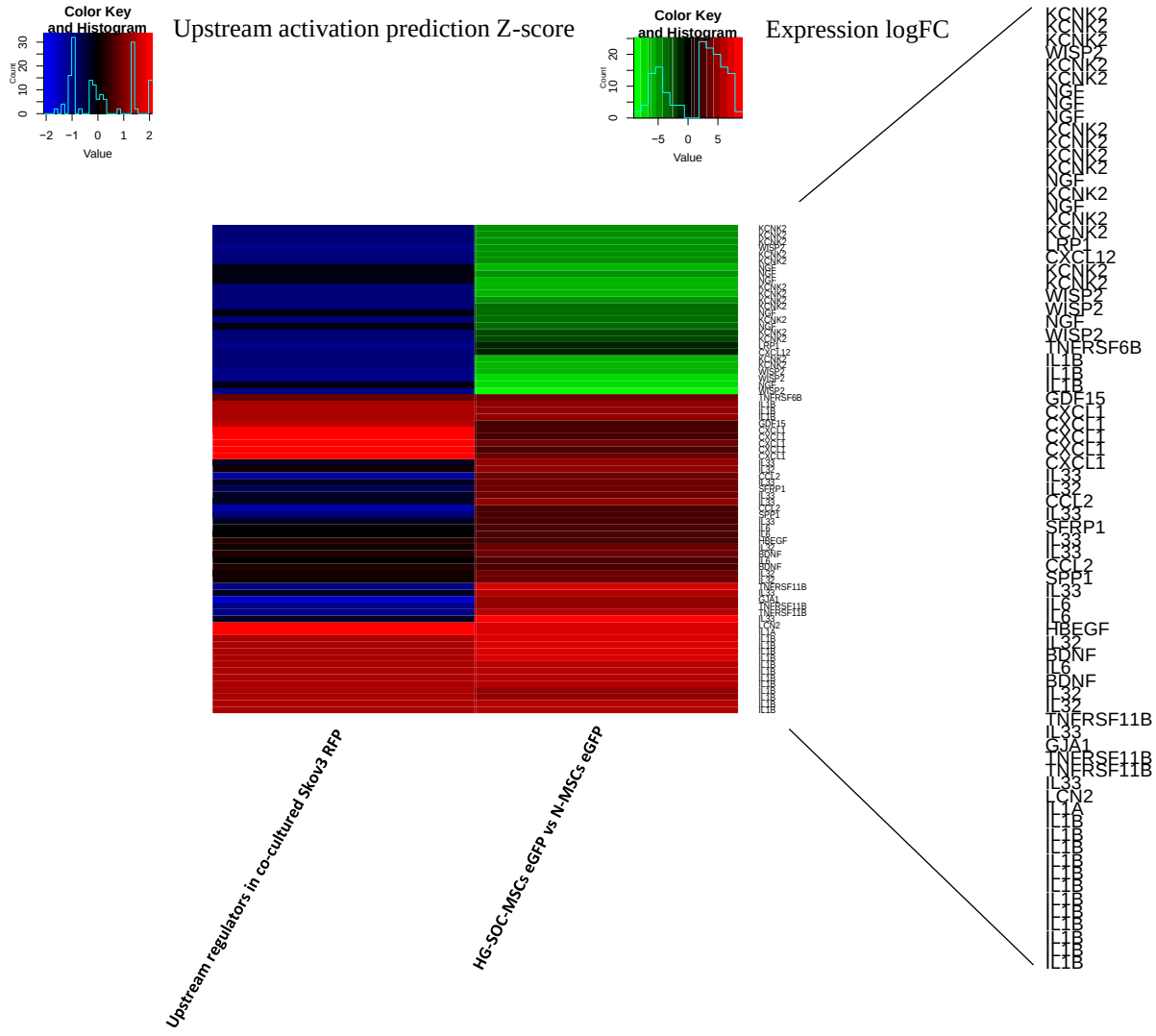

Figure 13. Heatmap of predicted upstream regulators delta activation Z-scores in co-cultures and expression logFC in HG-SOC-MSCs eGFP versus N-MSCs eGFP. The delta z-scores are obtained subtracting the predicted z-score of Skov3 RFP after N-MSCs eGFP co-culltures from the predicted z-score of Skov3 RFP after HG-SOC-MSCs eGFP co-cultures. Since differentially expression data have been obtained from the Fantom5 project using deepCage analysis, rows with the same gene symbol represent different TSS of the same gene.

We wanted to further investigate the possible interactions between the cellular populations by introducing the use of protein-protein interaction data. We used a compartmentalized protein-protein dataset (Veres et al., 2015) and selected exclusively interaction happening at the membrane level.

Fig 14 shows pairs of proteins/genes (A and B) that are predicted as regulators in the co-cultures, differentially expressed in HG-SOC-MSCs vs N-MSCs and can physically interact at the level of the membrane. This approach is more convoluted than the previous one and has the aim of explaining the observed transcriptional program in Skov3 co-cultured with MSCs through the identification of protein-

protein interaction altered in HG-SOC-MSCs respect to N-MSCs. All the protein pairs showed in Figure 14 represent protein-protein interaction happening at the membrane level altered in HG-SOC-MSCs that can possibly explain the peculiar transcriptional program of Skov3 after HG-SOC-MSCs co-culture. The study of the membrane protein-protein interaction will help us to highlight the interactor candidates, potentially responsible for the contact-dependent Skov3 remodeling in our co-culture model.

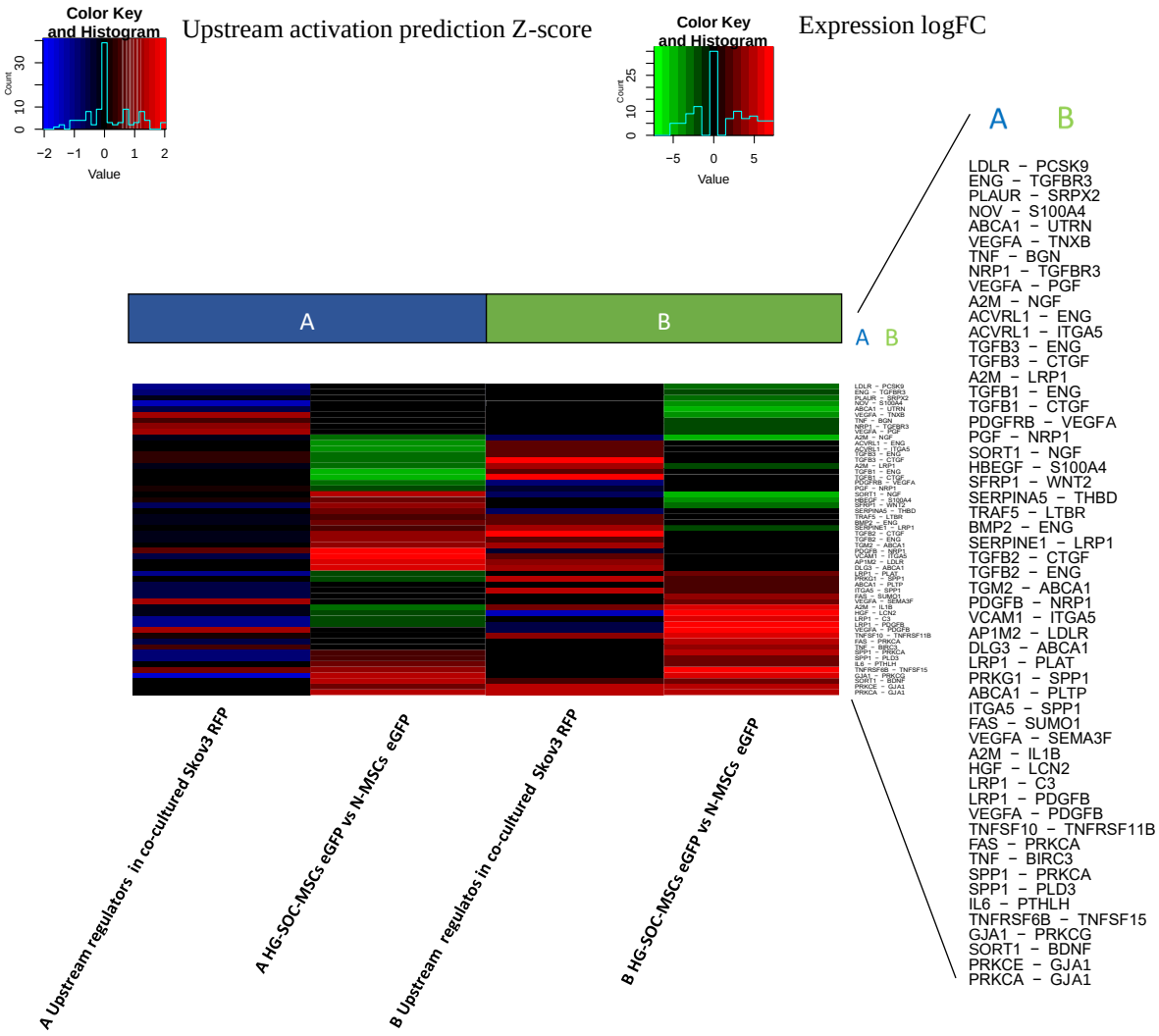

Figure 14.Heatmap of membrane protein-protein interactions upstream prediction and differential gene expression. Each row represents a pair of proteins (A and B) that can physically interact at the level of the membrane. For each protein/gene of the pair predicted, upstream regulators delta activation Z-scores in co-cultures and expression logFC in HG-SOC-MSCs eGFP versus N-MSCs eGFP are shown. The delta z-scores are obtained subtracting the predicted z-score of Skov3 RFP after N-MSCs co-cultures from the predicted z-score of Skov3 RFP after HG-SOC-MSCs eGFP co-cultures.

Gene set enrichment analysis reveals that the genes included in the altered membranome-interaction-network are involved in several critical pathways (table 6) that can be connected to the short-term co-culture data (both transcriptional-remodeling and phenotypic assays) with respect to:

1) altered-adhesion (Focal adhesion, Beta1 and Beta2 integrin activation together with hemostasis, platelet-activation) that altogether might stabilize adhesion-independent survival in combination to the recruitment of platelet/megakaryocites after exfoliation/dissemination from the primary-tumor-niche (see discussion)

2) altered MAPK and p38 signaling, pointing to maintenance of an altered MAPK/p38 balance (low-MAPK/high p38), which has been established as a critical intrinsic pathway to attain cancer-cell-dormancy (see discussion and (Adam et al., 2009) (Aguirre Ghiso et al., 1999) (Aguirre-Ghiso et al., 2003) (Aguirre-Ghiso et al., 2001) (Bragado et al., 2013) (Najmi et al., 2005) (Ruppender et al., 2015) (Sosa et al., 2011)).

3) altered signal transduction through IL1R and Cytokine and Inflammatory response as a general/common response to changed-microenvironment.

In addition, altered TGF-beta signaling pathway might be connected with p38-signaling pathway (Linde et al., 2016) since in the transcriptional remodeling of HG-SOC-MSCs with respect to N-MSCs we can observe an up-regulation of TGBF2 and a down-regulation of TGFB1 and TGFB3 and all three genes are critical in the normal physiology of ovarian development (Li, 2014)

Gene Set	FDR q-value
Genes involved in Hemostasis	8.80E-16
MAPK signaling pathway	5.88E-13
Focal adhesion	9.14E-13
Genes involved in Platelet activation, signaling and aggregation	1.20E-12
Signal transduction through IL1R	7.52E-10
Beta1 integrin cell surface interactions	3.72E-08
Cytokines and Inflammatory Response	3.72E-08
TGF-beta signaling pathway	1.51E-07
VEGFR1 specific signals	1.86E-06
Beta2 integrin cell surface interactions	2.67E-06
p38 MAPK Signaling Pathway	4.44E-04
Genes involved in NGF signaling via TRKA from the plasma membrane	7.15E-04
Intestinal immune network for IgA production	7.15E-04
Genes involved in Metabolism of lipids and lipoproteins	9.54E-04
Role of Calcineurin-dependent NFAT signaling in lymphocytes	9.83E-04

Table 6: GSEA analysis of predicted altered genes in our membranome interaction model

4.8. RT-qPCR validation of selected genes differentially expressed in Skov3 cells following long-term co-culture with HG-SOC-MSCs

A restricted set of genes upregulated in Skov3 RFP upon co-culture with HG-SOC-MSCs was selected for validation in RT-qPCR. We observed that the expression levels were more significantly increased by co-culture with HG-SOC-MSCs with respect to co-culture with N-MSCs or even less with membrane-separated co-culture with HG-SOC-MSCs.

In particular, these genes are IL8, CXCL1, CXCL2 and TNF (involved in the interleukin-10 signaling pathway), two members of the CCN family, namely CTGF and CYR61 (established YAP/TAZ target genes), in addition to FOS, EGR1 and ATF4, all in the category of immediate-early genes (fig. 15). It can be noticed that the differential regulation of the validated genes is present, at lower levels, also in the co-culture with N-MSC thus pointing to a quantitative-scaling response permitted by the dynamic-range limits of the responding system. It is worth reminding that also the differential transcriptome results comparing HG-SOC-MSC with N-MSCs, can be explained by a quantitative scaling within the allowed dynamic-range limits. The lowest differential response observed when performing membrane-separated co-culture points to the request of physical cell-to-cell contact for the maximal response efficiency.

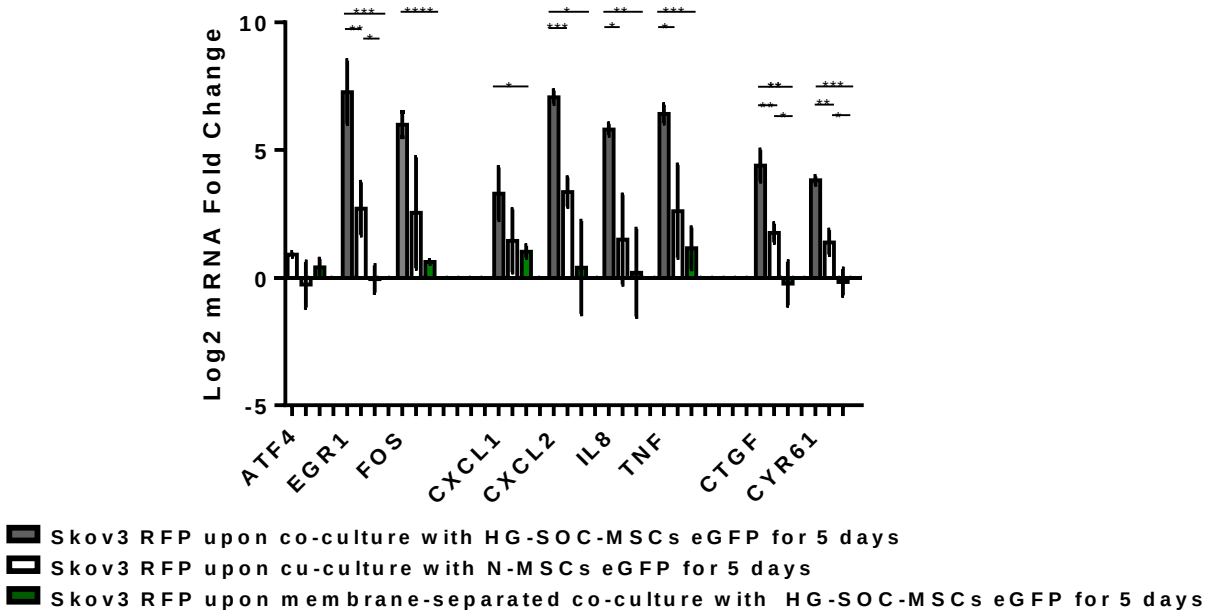

Figure 13. RT-qPCR validation showed that the selected set of genes are upregulated when long-term co-cultured with HG-SOC-MSCs eGFP, compared to N-MSCs eGFP or to a membrane-separated co-culture with HG-SOC-MSCs eGFP.

4.9 HG-SOC-MSCs are able to increase kinetics of tumor growth *in vivo*

In order to study if HG-SOC-MSCs may impact the *in vivo* growth of Skov3-induced tumor xenografts, we performed *in vivo* co-injection experiments. To this purpose we injected subcutaneously into NOD-SCID mice Skov3 cells only (n=15) or Skov3 cells admixed with HG-SOC-MSCs and previously co-cultured for 5 days (n=16). Once a primary tumor was detected, its growth was monitored until the tumor had reached 1 cm in diameter, and the animal was sacrificed. As shown in figure 16, the addition of HG-SOC-MSCs (red line) significantly enhanced the growth of the Skov3-induced tumor xenografts, as related to tumors induced by the injection of Skov3 alone (blue line) ($p>10^{-4}$). On the other hand, the same number of HG-SOC-MSCs alone injected subcutaneously into NOD-SCID mice (N=8) did not give rise to tumor formation (green line)

A

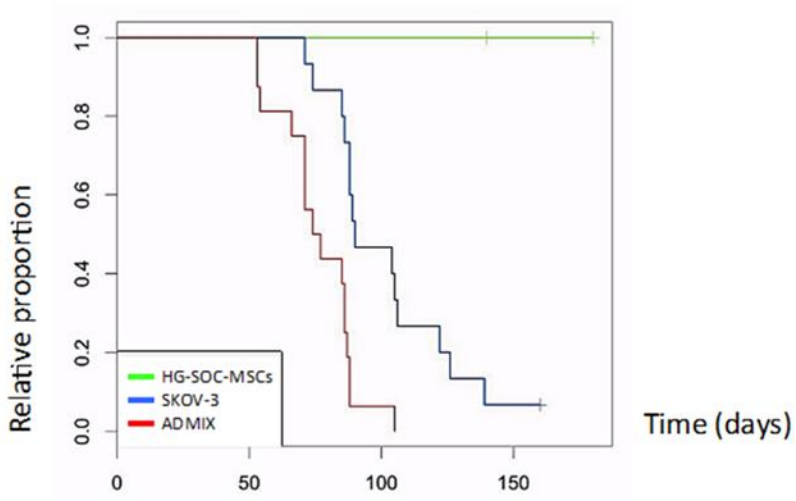

B

n	HG-SOC-MSCs	SKOV-3	Results
8	$2*10^5$---$4*10^5$		NO-tumors
15		$2*10^5$	Slow-growing tumors
16	$2*10^5$	$2*10^5$	Aggressive tumors

Figure 16. A. Kaplan-Meier plots for *in vivo* experiment. Green line represents mice injected subcutaneously with HG-SOC-MSCs only. Blue line represents mice injected subcutaneously with Skov3 only and red line represents mice injected with an admix (HG-SOC-MSCs, Skov3, ratio 1:1) B. Summary table of the mice and the cells injected.

4.10 The intrinsic differential-transcriptional dynamic-range of normal/cancer-derived MSC-compartment and its relevance to long-term co-culture cancer-cell-response.

The effects of long-term co-culture exerted by MSCs derived from tumor-tissue are still present, albeit at a significantly lower level, when MSCs derived from normal-tissues are used. We have previously demonstrated that transcriptional differences between N-MSCs and HG-SOC-MSCs are quantitative rather than qualitative (Verardo et al., 2014), evidencing that such differences are common within the limits of an established dynamic-range system. Similarly when comparing the transcriptional response of Skov3 to long-term-co-culture with N-MSC and HG-SOC-MSCs, the signature of differentially expressed genes is common and the differential quantitative response is still present albeit significantly less pronounced in the case of co-culture with N-MSCs (see Fig.15).

It was recently demonstrated (Bartosh et al., 2016) that bone-marrow MSCs are able to remodel the transcriptional program of breast cancer cells in 3D co-culture system. When comparing their results with our ovarian 2D co-culture model, we identify a common gene signature (fig.17). Among the 35 most upregulated (>10FC) genes in breast cancer cells after 3D co-culture with MSCs, 12 of them are also upregulated in our long-term co-culture model with HG-SOC-MSCs. Furthermore, this shared transcriptional program includes genes such as IL6, IL8, CXCL2, CXCL1, IL1B, FOSB, EGR1 and NFKBIZ. It is interesting to note that, although they use N-MSCs, such common signature is also induced when using HG-SOC-MSCs in our 2D-co-culture model.

Given this observation we are now performing preliminary studies looking at the possible role of N-MSCs in a more general context. To make the observed effects replicable in our 2D co-culture system we are using the same TNBC breast cancer-derived cell line (MDA-MB-231) in co-culture with the N-MSCs that we have used for the Skov3 cell-line

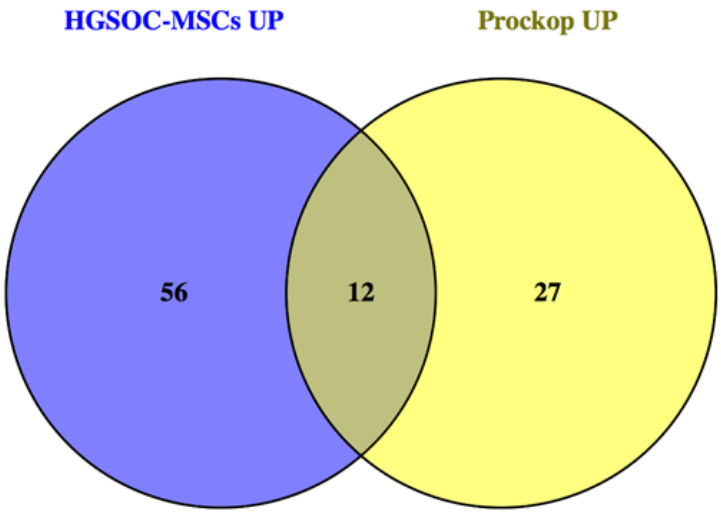

Figure 17 Overlap of genes up-regulated in Skov3 co-cultured with HG-SOC-MSC and genes up-regulated in MDA-MB-231 co-cultured in 3D model with MSCs as showed in (Bartosh et al., 2016).

4.11 WT1 as potential master-regulator in MSCs responsible for the dynamic-range of the MSC-intrinsic/extrinsic microenvironmental signaling.

The hypothesis we are investigating is that the mechanism responsible for the differential transcriptomic-remodeling in HG-SOC-MSCs with respect to N-MSC could be causally linked to the differential response of Skov3. Such mechanism should relate to the system level dynamic-range of the gene-regulatory-circuits within MSCs.

Since Wilms tumor 1 (WT1) was one of the genes found highly differentially expressed between HG-SOC-MSCs and N-MSCs *(average-fold-change 40)* (Verardo et al., 2014), we decided to test if it could play a regulatory role in our co-culture system. Indeed, when short-term co-culture was performed on a layer of HG-SOC-MSCs eGFP silenced for WT1, the viability of sorted Skov3 RFP cells was comparable to that measured in the controls (Skov3 RFP on homo-layer and on N-MSCs). On the contrary, the co-culture for 1 hour with HG-SOC-MSCs siControl generated an increased Skov3 RFP viability (Fig 18 A).

Moreover, it has been shown that the downregulation of the expression of WT1 in HG-SOC-MSCs eGFP is associated with a decreased mRNA level of leucine-rich repeat neuronal protein 4, LRRN4, which is

a type I transmembrane protein (Fig 18 B). Interestingly, LRRN4 is one of the differentially expressed genes between HG-SOC-MSCs and N-MSCs in the mesothelial-related gene signature, as reported in the introduction.

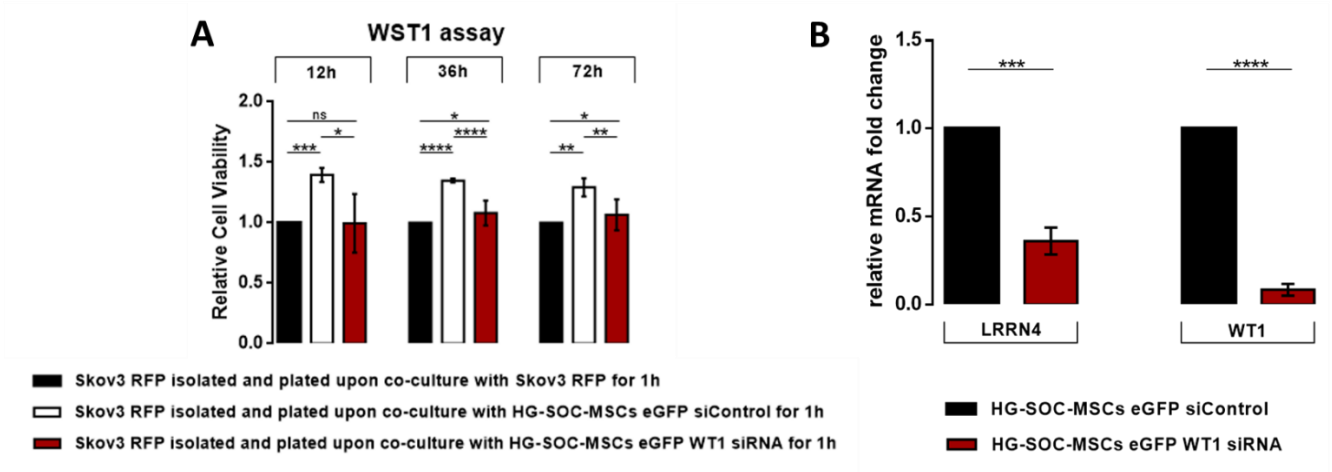

Figure 18. A) Viability assay of Skov3 RFP isolated and plated at different time points (12, 36, 72 hours) upon short-term co-culture with Skov3 RFP (black bars), HG-SOC-MSCs eGFP siControl (white bars), HG-SOC-MSCs eGFP WT1 siRNA (red bars), showed that WT1 expression in HG-SOC-MSCs is important to sustain an augmented viability of Skov3 RFP. B) Silencing of WT1 in HG-SOC-MSCs implicates the significant down regulation of LRRN4.

Preliminary data of gene expression profile analysis by DNA microarrays on HG-SOC-MSCs silenced for WT1 show how the suppression of WT1 transcription is able to revert part of the transcriptional program observed in HG-SOC-MSCs to the levels of expression of N-MSCs. In particular, pathways regulated by HMGB1, IL8 and IL6, all involved in inflammatory response, are more activated in HG-SOC-MSCs with respect to N-MSCs and are significantly suppressed after silencing of WT1 in HG-SOC-MSCs (table 7). We are replicating the observed preliminary results for implementing the statistical significance of the obtained data to confirm the relevance of WT1 in the cross-talk originating in the MSC-compartment.

Canonical Pathway	siWT1 HG-SOC-MSCs vs siControl HG-SOC-MSCs Z-score	HG-SOC-MSCs vs N-MSCs Z-score
HMGB1 Signaling	-1,41	2,29
IL-8 Signaling	-1,41	3,02
Gaq Signaling	-1,34	1,81
Cholecystokinin/Gastrin-mediated Signaling	-0,82	1,70
Signaling by Rho Family GTPases	-1,34	2,41
IL-6 Signaling	-0,82	1,34
Production of Nitric Oxide and Reactive Oxygen Species in Macrophages	-1,63	1,79
Th1 Pathway	-0,45	1,89
Integrin Signaling	-1,13	1,80
HGF Signaling	-0,45	1,41
Endothelin-1 Signaling	-0,45	1,09

Table 7. WT1 seems to be significant for some important pathway regulation in HG-SOC-MSCs. Positive values mean that the pathway is more expressed in HG-SOC-MSCs than in N-MSCs and negative values mean that pathways are more expressed in siControl HG-SOC-MSCs than in siWT1 HG-SOC-MSCs. Deltas of activation Z-scores are shown.

5. Discussion

During the work of my thesis we decided to take advantage of a simplified heterogeneous cell model system in which an ovarian cancer-derived cell line (Skov3 stably expressing RFP) was co-cultured with MSCs (N-MSCs or HG-SOC-MSCs stably expressing eGFP), in order to mimic the tumor-stroma interaction in High-Grade Serous Ovarian Cancer initiation and progression.

We investigated the transcriptional and functional relevance of the crosstalk between the two cell types at different time points (1 hour and 5 days of co-culture) and the influence that this interaction can exert on the tumor formation as assessed by the *in vivo* studies.

Certainly, even though the obtained results are promising and support the hypothesis at the base of this thesis, the range of clinical samples is too limited and the collected data need to be corroborated by a greater number of observations, especially considering the extreme heterogeneity of the high-grade serous ovarian cancer.

REQUIREMENT FOR CELL-TO-CELL CONTACT FOR BOTH TRANSCRIPTIONAL-REMODELLING AND PHENOTYPIC RESPONSE.

We proved that direct contact between the two cell types (starting from 1 hour of transient co-culture) is needed in order to induce a transcriptional remodeling and impact the functional behavior of Skov3 cells. In fact, short-term co-culture with HG-SOC-MSCs specifically affected Skov3 cells at different levels: 1) higher expression of four genes (ALDH1A3, IL1β, PDPN and MT1E), all involved in tumor progression through activating inflammation or migration/invasion pathways; 2) augmented viability; 3) increased motility and 4) greater tumorigenicity. Such altered behavior in Skov3 cells occurred only when the short-term co-culture was performed in a transient direct contact with HG-SOC-MSCs, but not with N-MSCs or by plating Skov3 cells in HG-SOC-MSCs conditioned medium for 1 hour. This could mean that the soluble factors released by HG-SOC-MSCs are not sufficient, or the timing is too short, to allow the proper secretion of extracellular factors and induce the observed phenotypes in Skov3 cells via specific receptor-ligand interaction between the two cell types.

We cannot exclude that a similar phenotypic response could be induced by N-MSC by lengthening the interaction time, since our experimental settings is limited to 1 hour.

The critical importance for direct contact is highlighted also by the results obtained at 5 days co-culture. RT-qPCR validation of selected genes identified by microarray analysis showed that they are strongly upregulated in Skov3 cells upon direct 5 days co-culture with HG-SOC-MSCs specifically, and less or even down regulated respectively upon direct co-culture with N-MSCs or with a membrane-separated system of co-culture with HG-SOC-MSCs. This data confirms and sustains our point regarding the importance of direct cell-contact-mediated-communication.

Different set of genes are upregulated in Skov3 cells upon co-culture/contact with HG-SOC-MSCs at 1 hour and 5 days, although some functional themes such as inflammation and migration are in common.

Obviously both the different experimental settings (in the short-term co-culture Skov3 are plated on HG-SOC-MSCs layer and collected after 1 hour while in the long-term co-culture, the two cell populations are kept together for 5 days before analysis) and the kinetics of gene-networking integration response are at the basis of the transcriptional remodeling.

THE SHORT-TERM-CO-CULTURE SIGNATURE; ANOIKIS-RESISTANCE FOR ENTRY INTO DORMANCY.

It is known that cancer-derived mesenchymal cells may contribute to the metastatic phenotype. The majority of tumor cells use the bloodstream to spread through the body whereby only a small fraction of tumor cells that have entered the circulatory system survive and extravasate to form metastases (Strilic and Offermanns, 2017). Once tumor cells detach from the primary tumor to enter the bloodstream they are exposed to various stresses through the loss of integrin-mediated adhesion to the extracellular matrix that is required for cell survival and can lead to programmed cell death, a process called “anoikis”. In addition, they are exposed to a normally operating immune system, which compared with the milieu of the primary tumor is not suppressed and able to efficiently attack and destroy tumor cells. Once shed from primary tumor, cancer cells use various mechanisms to inhibit anoikis (Buchheit et al., 2014) and protect against attack of the immune system: a common way of physical protection of tumor cells is the formation of tumor cell spheroids and tumor cell-platelet micro-aggregates, which results in the physical shielding of circulating tumor cells (Stegner et al., 2014). Such ‘protection’ mechanisms are overtly used for metastatic dissemination through hematogenous and lympatogenous pathways by forming the so-called ‘early-metastatic niche’ for subsequent trafficking to the final ‘implantation’ compartment. Some tumors use, as in the case of ovarian cancer, the transcoelomic route for local peritoneal dissemination using the mesothelial coelomic as target compartment. Here again the primary tumor ‘pre-metastatic niche’ is responsible for programming the sequential steps for development of resistance to anoikis,

formation of multicellular aggregates, transport in the peritoneal fluid, and final implantation into the peritoneum for growth as nodules (Weidle et al., 2016). Such protection mechanisms should already be programmed within the primary tumor 'pre-metastatic niche', that is before cells are shed to enter the circulation or the pelvic cavity. Among the genes found to be differentially expressed in Skov3 cells upon short-term co-culture with HG-SOC-MSCs there was PDPN. Human podoplanin is a type-1 transmembrane glycoprotein: its extracellular domain is known to bind the C-type lectin-like receptor 2 (CLEC2) expressed on platelets. As a result of its binding to CLEC2 on platelets, PDPN induces platelet aggregation and thereby promotes hematogenous metastasis. In addition to activating CLEC2, PDPN is known to form a complex with members of the ezrin-radixin-moesin (ERM) protein family, activate RhoA, inhibit anoikis and increase cell motility (Takeuchi et al., 2017). Another communication mechanism involves interaction either with TLR4 on platelets or CXCR4 in other stromal accessory cells for interacting with tumor cell-released high-mobility group box1 protein with the respectively HMGB1 cysteine-disulphide or reduced isoforms (this last forming an heterocomplex with CXCL12) (Yu et al., 2014). Therefore, the initial crosstalk within the primary-tumor 'pre-metastatic niche' is responsible for the programming shed cancer cells to activate subsequent interactions with available cellular components to form multicellular-aggregates that become resistant to anoikis and the attack of cell-based immunity. Crosstalk mechanisms in the primary tumor between cancer cells and normal stromal components, such as mesenchymal-stem cells, use common reciprocal interaction-based mechanisms, including platelets as associating vehicles, to self-sustain propagation of such aggregates to reach the acceptor compartment either endothelial or mesothelial linings and activate the invasive-program for the next round of transportation in the blood to the final destination or for direct implantation. In this perspective, the recent report by Sood group (Haemmerle et al., 2017) has highlighted the ability of ovarian cancer cell-lines to exploit platelets for reducing anoikis, through YAP1 activation, thereby promoting in vivo metastasis. We are exploiting our data showing that PDPN is highly expressed by Skov3 cells within 1 hour of contact with HG-SOC-MSCs.

THE LONG-TERM-CO-CULTURE Skov3 SIGNATURE: MAINTENANCE OF CANCER-CELL DORMANCY.

Mammalian adult stem cells are maintained in a physiological state of dormancy until appropriate signals, such as the loss of mature cells or the generation of a wound, trigger their proliferation. Dormancy not only is observed in physiological situations, but also is known to play a key role in the course of cell transformation and tumor progression. Disseminated tumor cells (DTCs) are capable to survive in a

dormant state whereby dormancy can be considered an adaptive response to microenvironmental stress. Several studies support the notion that DTCs enter a dormant state by being unable to establish appropriate interactions with the extracellular matrix (ECM) that support survival after infiltrating the parenchyma of metastatic target organs. The fact that tumor cells, which have disseminated/exfoliated from the primary tumor niche, enter quiescence and stop proliferating, but yet maintain reactivating capacity, should be the result of the crosstalk/combination of both intrinsic-cell-response-pathways and extrinsic-microenvironment-derived signals controlling the switch between DTC proliferation and dormancy. Several cancer cell-intrinsic signal pathways that lead to cellular dormancy have been described. Activation of the p38 MAPK pathway, coupled with decrease of mitogenic signals, has the net effect of promoting an $ERK^{low}/p38^{high}$ state in DTCs, which leads in turn to arrest in the G_0/G_1 phases of the cell cycle and associated quiescence. Historically, the balance between activated extracellular regulated kinase (ERK1/2) and activated p38α/β was the first signaling mechanism that has been connected reproducibly to DTC dormancy (Sosa et al., 2014) (Sosa et al., 2011). Our bioinformatics analysis has disclosed activation of the p38-pathway together with TGF-beta pathway; the validated gene-signature shows also the quantitative increase of ERG-genes including EGR1 and FOS, pointing to the regulatory network possibly buffering the mitogenic-MAPK path. Growth factors induced Ras/MAPK intracellular kinase cascade activates TFs at a first set of enhancers to initiate transcription of canonical early-response genes (ERGs). Many ERGs are TFs, such as AP-1 (*Fos*, *Fosb*, *Fosl1/2*, *Jun*, *Junb, EGR1*), which in turn regulate a late-response gene (LRG) program that mediates the cellular response to tissue damage (Galbraith and Espinosa, 2011). Importantly, Ras/MAPK signaling activates a similar set of ERGs in most cell types in the body, whereas LRGs tend to be highly cell-type specific. This suggests that ERG enhancer selection is not controlled by cell-type-specific TFs while LRG enhancer selection requires cell-type-specific TFs. The widespread expression of AP-1 TFs also suggests that they could participate in enhancer selection during the differentiation of many cell types, consistent with observations from previous studies (Heinz et al., 2013) (Hogan et al., 2017) (Maurano et al., 2015). To establish dormancy the LRG-enhancers should be blocked : EGR1-protein has been shown by Yamanaka group (Worringer et al., 2014)to be regulated via the Let7/LIN41 pathway,establishing EGR1 involvement in reprogramming blockade. It can therefore be hypothesized that increased TF-ERGs including EGR1 can establish maintenance of a ‘transcriptional-status-quo’ blocking reprogramming/differentiation and an active-metabolic state driven by buffered ERK1/2 path.

2D VERSUS 3D CO-CULTURES.

The co-culture models we have used are based on 2D cultures: in the last few years there has been a growing interest in using 3D culture platforms to understand the biology of MSCs (Cesarz and Tamama, 2016) (Ravi et al., 2015)(Sart et al., 2014) By mirroring natural conditions in vivo, 3D cultures are extremely useful for understanding complex interactions between different cellular populations and the matrix. Recently, the group of Prockop used 3D co-cultures of MSCs and breast cancer cells to demonstrate a possible mechanism of cancer cell cannibalism and activation of cancer cells dormancy promoted by N-MSCs derived from bone-marrow.(Bartosh et al., 2016). Transcriptome analysis revealed that cancer cells acquire a unique molecular signature enriched in pro-survival factors and inflammatory mediators with increased expression of Early Response Genes, including EGR1 and Fos Interestingly, comparing the transcriptomic data obtained from our co-cultures with that of the aforementioned 3D models, we can observe the activation of a similar transcriptional program. This suggest that the models we used, even though limited by the 2D approach, are able to enlighten a mechanism also present in 3D co-cultures and that this has a clinical relevance.

HG-SOC-MSCs AND N-MSCs: WT1 RELEVANCE IN SCALING THE DYNAMIC-RANGE OF THE COMMON SIGNATURE AND ITS EFFECT ON CROSS-TALK.

It is interesting to note that the HG-SOC-MSCs used in this study (Verardo et al., 2014) do not display any chromosomal aberration and are considered normal from a genomic point of view. The observed differential transcriptional signature between HG-SOC-MSC and N-MSC highlights the quantitative variation/scaling within a dynamic-range that should be buffered by epigenetic signaling coupled to master-gene regulatory networks. In this light, even though we could not find an effective molecular mechanism that may explain the phenotypes discovered in Skov3 cells upon short-term co-culture with HG-SOC-MSCs, we have hypothesized WT1 as a possible key player in the crosstalk. WT1 is a transcription factor strongly expressed in HG-SOC-MSCs, and at a significantly lower level in N-MSCs. Upon silencing of WT1 in HG-SOC-MSCs, we noticed a down-regulation of LRRN4, a transmembrane protein, which is generally expressed on HG-SOC-MSCs surface, but not in N-MSCs. Moreover, LRRN4 is a gene found to be upregulated in the HG-SOC-MSCs mesothelial-related gene signature that correlates with a bad prognosis in patients with HG-SOC (Verardo et al., 2014). LRRN4 may be involved, possibly via WT1, in the orchestration of the crosstalk between Skov3 and HG-SOC-MSCs at least when the two cell lines are short-term co-cultured. In order to confirm this hypothesis, we are currently setting

short term co-culture experiments between Skov3 and HG-SOC-MSCs silenced for LRRN4 to investigate its possible role in the tumor-stroma interaction.

CO-CULTURED AND ADMIXED Skov3/HG-SOC-MSCs SIGNIFICANTLY INCREASE THE KINETICS OF TUMOR GROWTH. We finally investigated the impact of MSCs in vivo: the in vivo experiments have shown that a subcutaneously co-injection into NOD-SCID mice of an admix of Skov3 and HG-SOC-MSCs (ratio 1:1), previously co-cultured for 5 days, resulted in an augmented kinetics of the Skov3-derived tumor growth when compared to the single cell lines injection. In fact, HG-SOC-MSCs alone injection resulted in no tumor formation, while a Skov3 alone injection displayed a slow growing tumor. This confirms the hypothesis that cancer-derived MSCs are able to establish a tumor-promoting environment as also confirmed in other systems with the use of N-MSCs. However, we know that human stroma can be substitute by the murine stromal cells, unless human stroma cells are necessary to support the tumor growth. For this reason, we will value the percentage of the residual human MSCs in the xenograft.

6. Future perspective and conclusions

MSCs are a deeply heterogeneous cell population that can be influenced by several stimuli such as the initial source and the environment in which they exert their functions. The distinction between the cancer-derived MSCs and normal tissue derived-MSCs is not clear and appear to be more quantitative than qualitative, as demonstrate also in the paper by Verardo et al., 2014 that highlighted a common transcriptional core in mesenchymal cell lines, with different quantitative levels. Interestingly, this thesis pointed out that the transcriptional remodeling of Skov3 upon co-culture with HG-SOC-MSCs and N-MSCs at different time points present a common transcriptional nucleus, more evident in consequence to the co-culture with HG-SOC-MSCs with respect to N-MSCs.

Altogether both our bioinformatics analysis together with the cluster-validated genes point to the activation and stabilization of a Skov3-dormancy-program (long-term-co-culture) strictly connected to an altered adhesion behavior potentially including platelet recruitment (short-term-co-culture) as associated to the exfoliation/dissemination request for anoikis-survival.

At a functional level, we would like to deeply investigate the functional role of N-MSCs in the crosstalk with ovarian cancer cells. Indeed, a limit of the short-term co-culture setting is the timing, that most likely obstruct N-MSCs to remodel Skov3. Moreover, we would like to perform co-culture experiments with different cancer cell lines in order to determine the observed remodeling specificity, since we already found out a general cluster of genes up-regulated both in our model and in a 3D co-culture model between bone-marrow MSCs and a breast cancer cell line (Bartosh et al., 2016) as observed in fig. 17.

Even though we perceived that HG-SOC-MSCs, in particular, are able to remodel Skov3 at a transcriptional and functional level, by conferring greater pro-tumorigenic abilities, and by increasing kinetics of tumor growth in mice xenograft *in vivo*, we could not trace back to a specific molecular mechanism. However, we focused our attention on WT1, a transcriptional factor differentially expressed between HG-SOC-MSCs and N-MSCs (Verardo et al., 2014). WT1 appears to be interesting because its transcriptional suppression in HG-SOC-MSCs leads to 1) the reinstatement of the viability of Skov3, taking it back to a similar viability obtained with N-MSCs co-culture; 2) the down-regulation of LRRN4 gene, which is a type I transmembrane protein. LRRN4 is another differentially expressed genes between HG-SOC-MSCs and N-MSCs in the mesothelial-related gene signature, as reported in the introduction, and it is associated with a poor clinical prognosis (Verardo et al., 2014); 3) the preliminary partial reversion of the transcriptional program observed in HG-SOC-MSCs to the N-MSCs expression levels.

For these reasons, we would like to better investigate the potential role of WT1 in orchestrating the cross-talk originating in the MSC-compartment.

As shown in Fig. 7, the upregulation of Podoplanin (PDPN) in Skov3 cells after short-term co-culture with HG-SOC-MSCs is both very strong (153 fold-induction) and very selective. It is known that in lymphatic endothelial cells (LECs), PDPN activates platelets by binding to CLEC-2, acting as a developmental conduit to blood/lymphatic vessel separation. Platelets activation by exfoliated cancer cells is also critical in promoting hematogenous metastasis (Suzuki-Inoue et al., 2017). Therefore the cross-talk within the primary-tumor 'pre-metastatic-niche', involving the HG-SOC-MSCs compartment, could be responsible for programming shed cancer cells to subsequently activating interactions, i.e. with platelets, to form multicellular-aggregates that become resistant to anoikis and acquiring increased spreading ability. In this perspective a recent report from Sood group (Haemmerle et al, 2017) has highlighted the ability of ovarian cancer cell lines to exploit platelets for reducing anoikis through YAP1 activation.

To understand whether PDPN might represent a critical transducer of platelet recruitment I am currently investigating the following experimental points:

1) Validation of the kinetics of PDPN-protein expression after short-term co-culture with HG-SOC-MSC both for Skov3 and other ovarian and TNBC cell-lines (negative-control being the respective cell-line) to understand whether the observed regulation is cell line-dependent or more general.

2) Evaluation of PDPN functional activity in the selected phenotypic assays via PDPN-siRNA.

3) Role of PDPN activity in regulating YAP1 activation/nuclear shuttling and phosphorylation levels via PDPN-siRNA.

As already mentioned in the discussion, the results collected during my PhD project are interesting and promising, but not conclusive. It is known that High-Grade Serous Ovarian Carcinoma is one highly heterogeneous subtype of cancer and, for this reason, to confirm our data, it will be necessary to increase the number of the clinical samples and the spectrum of observations. Furthermore, it will be fundamental to strengthen the observations by using several ovarian carcinoma cell lines.

Moreover, as sketched in the results chapter, we focused strongly on the hypothesis that Skov3 are phenotypically remodeled by a specific induction mediated by the HG-SOC-MSCs layer when related to N-MSCs, upon short term co-culture. However, since HG-SOC-MSCs are able to attract more Skov3 to their layer when compared to N-MSCs, it has to be considered the hypothesis that our results can also be due to a selection of Skov3 mediated by HG-SOC-MSCs with respect to N-MSCs. Thus, Skov3 adhered to the HG-SOC-MSCs layer could be different, at a phenotypic level, respect to the not adhered

population. To validate this hypothesis, we are planning to monitor the expression of PDPN in Skov3 upon short term co-culture with HG-SOC-MSCs and to verify if the levels of PDPN are equally augmented in both the two Skov3 populations (adhered to the layer or still in suspension) or if there is any difference at an expression level among them.

7. Bibliography

(DGT), T.F.C. and the R.P. and C., Forrest, A.R.R., Kawaji, H., Rehli, M., Baillie, J.K., Hoon, M.J.L. de, Haberle, V., Lassmann, T., Kulakovskiy, I. V., Lizio, M., et al. (2014). A promoter-level mammalian expression atlas. Nature *507*, 462–470.

Adam, A.P., George, A., Schewe, D., Bragado, P., Iglesias, B. V., Ranganathan, A.C., Kourtidis, A., Conklin, D.S., and Aguirre-Ghiso, J.A. (2009). Computational Identification of a p38SAPK-Regulated Transcription Factor Network Required for Tumor Cell Quiescence. Cancer Res. *69*, 5664–5672.

Aguirre-Ghiso, J.A., Liu, D., Mignatti, A., Kovalski, K., and Ossowski, L. (2001). Urokinase receptor and fibronectin regulate the ERK(MAPK) to p38(MAPK) activity ratios that determine carcinoma cell proliferation or dormancy in vivo. Mol. Biol. Cell *12*, 863–879.

Aguirre-Ghiso, J.A., Estrada, Y., Liu, D., and Ossowski, L. (2003). ERK(MAPK) activity as a determinant of tumor growth and dormancy; regulation by p38(SAPK). Cancer Res. *63*, 1684–1695.

Aguirre Ghiso, J.A., Kovalski, K., and Ossowski, L. (1999). Tumor dormancy induced by downregulation of urokinase receptor in human carcinoma involves integrin and MAPK signaling. J. Cell Biol. *147*, 89–104.

Ahmed, A.A., Etemadmoghadam, D., Temple, J., Lynch, A.G., Riad, M., Sharma, R., Stewart, C., Fereday, S., Caldas, C., deFazio, A., et al. (2010). Driver mutations in TP53 are ubiquitous in high grade serous carcinoma of the ovary. J. Pathol. *221*, 49–56.

Allavena, P., Sica, A., Garlanda, C., and Mantovani, A. (2008). The Yin-Yang of tumor-associated macrophages in neoplastic progression and immune surveillance. Immunol. Rev. *222*, 155–161.

Alsop, K., Fereday, S., Meldrum, C., deFazio, A., Emmanuel, C., George, J., Dobrovic, A., Birrer, M.J., Webb, P.M., Stewart, C., et al. (2012). *BRCA* Mutation Frequency and Patterns of Treatment Response in *BRCA* Mutation–Positive Women With Ovarian Cancer: A Report From the Australian Ovarian Cancer Study Group. J. Clin. Oncol. *30*, 2654–2663.

Ame-Thomas, P., Maby-El Hajjami, H., Monvoisin, C., Jean, R., Monnier, D., Caulet-Maugendre, S., Guillaudeux, T., Lamy, T., Fest, T., and Tarte, K. (2007). Human mesenchymal stem cells isolated from bone marrow and lymphoid organs support tumor B-cell growth: role of stromal cells in follicular lymphoma pathogenesis. Blood *109*, 693–702.

Ammirante, M., Luo, J.-L., Grivennikov, S., Nedospasov, S., and Karin, M. (2010). B-cell-derived lymphotoxin promotes castration-resistant prostate cancer. Nature *464*, 302–305.

Arai, F., Hirao, A., Ohmura, M., Sato, H., Matsuoka, S., Takubo, K., Ito, K., Koh, G.Y., and Suda, T. (2004). Tie2/Angiopoietin-1 Signaling Regulates Hematopoietic Stem Cell Quiescence in the Bone Marrow Niche. Cell *118*, 149–161.

Baratta, M.G., Schinzel, A.C., Zwang, Y., Bandopadhayay, P., Bowman-Colin, C., Kutt, J., Curtis, J., Piao, H., Wong, L.C., Kung, A.L., et al. (2015). An in-tumor genetic screen reveals that the BET bromodomain protein, BRD4, is a potential therapeutic target in ovarian carcinoma. Proc. Natl. Acad. Sci. U. S. A. *112*, 232–237.

Bartosh, T.J., Ullah, M., Zeitouni, S., Beaver, J., and Prockop, D.J. (2016). Cancer cells enter dormancy after cannibalizing mesenchymal stem/stromal cells (MSCs). Proc. Natl. Acad. Sci. U. S. A. *113*, E6447–E6456.

Bayne, L.J., Beatty, G.L., Jhala, N., Clark, C.E., Rhim, A.D., Stanger, B.Z., and Vonderheide, R.H. (2012). Tumor-Derived Granulocyte-Macrophage Colony-Stimulating Factor Regulates Myeloid Inflammation and T Cell Immunity in Pancreatic Cancer. Cancer Cell *21*, 822–835.

Bell, D., Berchuck, A., Birrer, M., Chien, J., Cramer, D.W., Dao, F., Dhir, R., DiSaia, P., Gabra, H., Glenn, P., et al. (2011). Integrated genomic analyses of ovarian carcinoma. Nature *474*, 609–615.

Bissanum, R., Lirdprapamongkol, K., Svasti, J., Navakanitworakul, R., and Kanokwiroon, K. (2017). The role of WT1 isoforms in vasculogenic mimicry and metastatic potential of human triple negative breast cancer cells. Biochem. Biophys. Res. Commun. *494*, 256–262.

Bragado, P., Estrada, Y., Parikh, F., Krause, S., Capobianco, C., Farina, H.G., Schewe, D.M., and Aguirre-Ghiso, J.A. (2013). TGF-β2 dictates disseminated tumour cell fate in target organs through TGF-

β-RIII and p38α/β signalling. Nat. Cell Biol. *15*, 1351–1361.

Brennen, W.N., Chen, S., Denmeade, S.R., and Isaacs, J.T. (2013). Quantification of Mesenchymal Stem Cells (MSCs) at Sites of Human Prostate Cancer. Oncotarget *4*, 106–117.

Buchheit, C.L., Weigel, K.J., and Schafer, Z.T. (2014). Cancer cell survival during detachment from the ECM: multiple barriers to tumour progression. Nat. Rev. Cancer *14*, 632–641.

Buckanovich, R.J., Facciabene, A., Kim, S., Benencia, F., Sasaroli, D., Balint, K., Katsaros, D., O'Brien-Jenkins, A., Gimotty, P.A., and Coukos, G. (2008). Endothelin B receptor mediates the endothelial barrier to T cell homing to tumors and disables immune therapy. Nat. Med. *14*, 28–36.

Butler, J.M., Nolan, D.J., Vertes, E.L., Varnum-Finney, B., Kobayashi, H., Hooper, A.T., Seandel, M., Shido, K., White, I.A., Kobayashi, M., et al. (2010). Endothelial Cells Are Essential for the Self-Renewal and Repopulation of Notch-Dependent Hematopoietic Stem Cells. Cell Stem Cell *6*, 251–264.

Cai, H., and Xu, Y. (2013). The role of LPA and YAP signaling in long-term migration of human ovarian cancer cells. Cell Commun. Signal. *11*, 31.

Calon, A., Espinet, E., Palomo-Ponce, S., Tauriello, D.V.F., Iglesias, M., Céspedes, M.V., Sevillano, M., Nadal, C., Jung, P., Zhang, X.H.-F., et al. (2012). Dependency of colorectal cancer on a TGF-β-driven program in stromal cells for metastasis initiation. Cancer Cell *22*, 571–584.

Calon, A., Tauriello, D.V.F., and Batlle, E. (2014). TGF-beta in CAF-mediated tumor growth and metastasis. Semin. Cancer Biol. *25*, 15–22.

Calvi, L.M., Adams, G.B., Weibrecht, K.W., Weber, J.M., Olson, D.P., Knight, M.C., Martin, R.P., Schipani, E., Divieti, P., Bringhurst, F.R., et al. (2003). Osteoblastic cells regulate the haematopoietic stem cell niche. Nature *425*, 841–846.

Caplan, A.I., and Correa, D. (2011). The MSC: An Injury Drugstore. Cell Stem Cell *9*, 11–15.

Carlson, J.W., Miron, A., Jarboe, E.A., Parast, M.M., Hirsch, M.S., Lee, Y., Muto, M.G., Kindelberger, D., and Crum, C.P. (2008). Serous Tubal Intraepithelial Carcinoma: Its Potential Role in Primary Peritoneal Serous Carcinoma and Serous Cancer Prevention. J. Clin. Oncol. *26*, 4160–4165.

Cesarz, Z., and Tamama, K. (2016). Spheroid Culture of Mesenchymal Stem Cells. Stem Cells Int. *2016*, 1–11.

Chamberlain, G., Fox, J., Ashton, B., and Middleton, J. (2007). Concise Review: Mesenchymal Stem Cells: Their Phenotype, Differentiation Capacity, Immunological Features, and Potential for Homing. Stem Cells *25*, 2739–2749.

Cheng, B., Lu, W., Xiaoyun, W., YaXia, C., and Xie, X. (2009). Extra-abdominal Metastases From Epithelial Ovarian Carcinoma. Int. J. Gynecol. Cancer *19*, 611–614.

Cho, J.A., Park, H., Lim, E.H., Kim, K.H., Choi, J.S., Lee, J.H., Shin, J.W., and Lee, K.W. (2011). Exosomes from ovarian cancer cells induce adipose tissue-derived mesenchymal stem cells to acquire the physical and functional characteristics of tumor-supporting myofibroblasts. Gynecol. Oncol. *123*, 379–386.

Corcoran, K.E., Trzaska, K.A., Fernandes, H., Bryan, M., Taborga, M., Srinivas, V., Packman, K., Patel, P.S., and Rameshwar, P. (2008). Mesenchymal Stem Cells in Early Entry of Breast Cancer into Bone Marrow. PLoS One *3*, e2563.

Cormio, G., Rossi, C., Cazzolla, A., Resta, L., Loverro, G., Greco, P., and Selvaggi, L. Distant metastases in ovarian carcinoma. Int. J. Gynecol. Cancer *13*, 125–129.

Costanza, B., Umelo, I., Bellier, J., Castronovo, V., and Turtoi, A. (2017). Stromal Modulators of TGF-β in Cancer. J. Clin. Med. *6*, 7.

Coussens, L.M., Raymond, W.W., Bergers, G., Laig-Webster, M., Behrendtsen, O., Werb, Z., Caughey, G.H., and Hanahan, D. (1999). Inflammatory mast cells up-regulate angiogenesis during squamous epithelial carcinogenesis. Genes Dev. *13*, 1382–1397.

Crum, C.P., Herfs, M., Ning, G., Bijron, J.G., Howitt, B.E., Jimenez, C.A., Hanamornroongruang, S., McKeon, F.D., and Xian, W. (2013). Through the glass darkly: intraepithelial neoplasia, top-down differentiation, and the road to ovarian cancer. J. Pathol. *231*, 402–412.

Cuiffo, B.G., and Karnoub, A.E. (2012). Mesenchymal stem cells in tumor development. Cell Adh. Migr. *6*, 220–230.

Direkze, N.C., Hodivala-Dilke, K., Jeffery, R., Hunt, T., Poulsom, R., Oukrif, D., Alison, M.R., and Wright, N.A. (2004). Bone Marrow Contribution to Tumor-Associated Myofibroblasts and Fibroblasts. Cancer Res. *64*, 8492–8495.

Dominici, M., Le Blanc, K., Mueller, I., Slaper-Cortenbach, I., Marini, F.., Krause, D.S., Deans, R.J., Keating, A., Prockop, D.J., and Horwitz, E.M. (2006). Minimal criteria for defining multipotent mesenchymal stromal cells. The International Society for Cellular Therapy position statement. Cytotherapy *8*, 315–317.

Dotto, G.P., Weinberg, R.A., and Ariza, A. (1988). Malignant transformation of mouse primary keratinocytes by Harvey sarcoma virus and its modulation by surrounding normal cells. Proc. Natl. Acad. Sci. U. S. A. *85*, 6389–6393.

Dubeau, L. (1999). The Cell of Origin of Ovarian Epithelial Tumors and the Ovarian Surface Epithelium Dogma: Does the Emperor Have No Clothes? Gynecol. Oncol. *72*, 437–442.

Duda, D.G., Duyverman, A.M.M.J., Kohno, M., Snuderl, M., Steller, E.J.A., Fukumura, D., and Jain, R.K. (2010). Malignant cells facilitate lung metastasis by bringing their own soil. Proc. Natl. Acad. Sci. *107*, 21677–21682.

Dutton, J.R., Lahiri, D., and Ward, A. (2006). Different isoforms of the Wilms' tumour protein WT1 have distinct patterns of distribution and trafficking within the nucleus. Cell Prolif. *39*, 519–535.

Dvorak, H.F. (2015). Tumors: Wounds That Do Not Heal--Redux. Cancer Immunol. Res. *3*, 1–11.

Fathalla, M.F. (1971). Incessant ovulation--a factor in ovarian neoplasia? Lancet (London, England) *2*, 163.

Friedenstein, A.J., Chailakhjan, R.K., and Lalykina, K.S. (1970). The development of fibroblast colonies in monolayer cultures of guinea-pig bone marrow and spleen cells. Cell Tissue Kinet. *3*, 393–403.

Fujita, H., Ohuchida, K., Mizumoto, K., Nakata, K., Yu, J., Kayashima, T., Cui, L., Manabe, T., Ohtsuka, T., and Tanaka, M. (2010). α-Smooth Muscle Actin Expressing Stroma Promotes an Aggressive Tumor Biology in Pancreatic Ductal Adenocarcinoma. Pancreas *39*, 1254–1262.

Gabrilovich, D.I., Ostrand-Rosenberg, S., and Bronte, V. (2012). Coordinated regulation of myeloid cells by tumours. Nat. Rev. Immunol. *12*, 253–268.

Galbraith, M.D., and Espinosa, J.M. (2011). Lessons on transcriptional control from the serum response network. Curr. Opin. Genet. Dev. *21*, 160–166.

Gentleman, R.C., Carey, V.J., Bates, D.M., Bolstad, B., Dettling, M., Dudoit, S., Ellis, B., Gautier, L., Ge, Y., Gentry, J., et al. (2004). Bioconductor: open software development for computational biology and bioinformatics. Genome Biol. *5*, R80.

Gilks, C.B., Irving, J., Köbel, M., Lee, C., Singh, N., Wilkinson, N., and McCluggage, W.G. (2015). Incidental Nonuterine High-grade Serous Carcinomas Arise in the Fallopian Tube in Most Cases. Am. J. Surg. Pathol. *39*, 357–364.

González-Reyes, S., Marín, L., González, L., González, L.O., del Casar, J.M., Lamelas, M.L., González-Quintana, J.M., and Vizoso, F.J. (2010). Study of TLR3, TLR4 and TLR9 in breast carcinomas and their association with metastasis. BMC Cancer *10*, 665.

Gronthos, S., Mankani, M., Brahim, J., Robey, P.G., and Shi, S. (2000). Postnatal human dental pulp stem cells (DPSCs) in vitro and invivo. Proc. Natl. Acad. Sci. *97*, 13625–13630.

Des Guetz, G., Uzzan, B., Nicolas, P., Cucherat, M., Morere, J.-F., Benamouzig, R., Breau, J.-L., and Perret, G.-Y. (2006). Microvessel density and VEGF expression are prognostic factors in colorectal cancer. Meta-analysis of the literature. Br. J. Cancer *94*, 1823–1832.

Haemmerle, M., Taylor, M.L., Gutschner, T., Pradeep, S., Cho, M.S., Sheng, J., Lyons, Y.M., Nagaraja, A.S., Dood, R.L., Wen, Y., et al. (2017). Platelets reduce anoikis and promote metastasis by activating YAP1 signaling. Nat. Commun. *8*, 310.

Hall, B., Andreeff, M., and Marini, F. (2007a). The Participation of Mesenchymal Stem Cells in Tumor Stroma Formation and Their Application as Targeted-Gene Delivery Vehicles. In Bone Marrow-Derived Progenitors, (Berlin, Heidelberg: Springer Berlin Heidelberg), pp. 263–283.

Hall, B., Dembinski, J., Sasser, A., Studeny, M., Andreeff, M., and Marini, F. (2007b). Mesenchymal Stem Cells in Cancer: Tumor-Associated Fibroblasts and Cell-Based Delivery Vehicles. Int. J. Hematol.

86, 8–16.

Hanahan, D., and Coussens, L.M. (2012). Accessories to the crime: functions of cells recruited to the tumor microenvironment. Cancer Cell *21*, 309–322.

Hanahan, D., and Weinberg, R.A. (2011). Hallmarks of cancer: the next generation. Cell *144*, 646–674.

Hanahan, D., Bergers, G., Brekken, R., McMahon, G., Vu, T.H., Itoh, T., Tamaki, K., Tanzawa, K., Thorpe, P., Itohara, S., et al. (2000). Matrix metalloproteinase-9 triggers the angiogenic switch during carcinogenesis. Nat. Cell Biol. *2*, 737–744.

Hegde, P.S., Jubb, A.M., Chen, D., Li, N.F., Meng, Y.G., Bernaards, C., Elliott, R., Scherer, S.J., and Chen, D.S. (2013). Predictive Impact of Circulating Vascular Endothelial Growth Factor in Four Phase III Trials Evaluating Bevacizumab. Clin. Cancer Res. *19*, 929–937.

Heinz, S., Romanoski, C.E., Benner, C., Allison, K.A., Kaikkonen, M.U., Orozco, L.D., and Glass, C.K. (2013). Effect of natural genetic variation on enhancer selection and function. Nature *503*, 487–492.

Hogan, N.T., Whalen, M.B., Stolze, L.K., Hadeli, N.K., Lam, M.T., Springstead, J.R., Glass, C.K., and Romanoski, C.E. (2017). Transcriptional networks specifying homeostatic and inflammatory programs of gene expression in human aortic endothelial cells. Elife *6*.

Horwitz, E.M., Le Blanc, K., Dominici, M., Mueller, I., Slaper-Cortenbach, I., Marini, F.C., Deans, R.J., Krause, D.S., Keating, A., and International Society for Cellular Therapy (2005). Clarification of the nomenclature for MSC: The International Society for Cellular Therapy position statement. Cytotherapy *7*, 393–395.

Hossain, A., Gumin, J., Gao, F., Figueroa, J., Shinojima, N., Takezaki, T., Priebe, W., Villarreal, D., Kang, S.-G., Joyce, C., et al. (2015). Mesenchymal Stem Cells Isolated From Human Gliomas Increase Proliferation and Maintain Stemness of Glioma Stem Cells Through the IL-6/gp130/STAT3 Pathway. Stem Cells *33*, 2400–2415.

Howitt, B.E., Hanamornroongruang, S., Lin, D.I., Conner, J.E., Schulte, S., Horowitz, N., Crum, C.P., and Meserve, E.E. (2015). Evidence for a Dualistic Model of High-grade Serous Carcinoma. Am. J. Surg. Pathol. *39*, 287–293.

Huang, D.W., Sherman, B.T., and Lempicki, R.A. (2008). Systematic and integrative analysis of large gene lists using DAVID bioinformatics resources. Nat. Protoc. *4*, 44–57.

Huang, J.I., Beanes, S.R., Zhu, M., Lorenz, H.P., Hedrick, M.H., and Benhaim, P. (2002). Rat extramedullary adipose tissue as a source of osteochondrogenic progenitor cells. Plast. Reconstr. Surg. *109*, 1033-41-3.

Jeon, E.S., Moon, H.J., Lee, M.J., Song, H.Y., Kim, Y.M., Cho, M., Suh, D.-S., Yoon, M.-S., Chang, C.L., Jung, J.S., et al. (2008). Cancer-Derived Lysophosphatidic Acid Stimulates Differentiation of Human Mesenchymal Stem Cells to Myofibroblast-Like Cells. Stem Cells *26*, 789–797.

Ji, J.F., He, B.P., Dheen, S.T., and Tay, S.S.W. (2004). Interactions of Chemokines and Chemokine Receptors Mediate the Migration of Mesenchymal Stem Cells to the Impaired Site in the Brain After Hypoglossal Nerve Injury. Stem Cells *22*, 415–427.

Junttila, M.R., and de Sauvage, F.J. (2013). Influence of tumour micro-environment heterogeneity on therapeutic response. Nature *501*, 346–354.

Kalluri, R. (2003). Angiogenesis: Basement membranes: structure, assembly and role in tumour angiogenesis. Nat. Rev. Cancer *3*, 422–433.

Kalluri, R. (2016). The biology and function of fibroblasts in cancer. Nat. Rev. Cancer *16*, 582–598.

Kansy, B.A., Dißmann, P.A., Hemeda, H., Bruderek, K., Westerkamp, A.M., Jagalski, V., Schuler, P., Kansy, K., Lang, S., Dumitru, C.A., et al. (2014). The bidirectional tumor - mesenchymal stromal cell interaction promotes the progression of head and neck cancer. Stem Cell Res. Ther. *5*, 95.

Kaplan, R.N., Riba, R.D., Zacharoulis, S., Bramley, A.H., Vincent, L., Costa, C., MacDonald, D.D., Jin, D.K., Shido, K., Kerns, S.A., et al. (2005). VEGFR1-positive haematopoietic bone marrow progenitors initiate the pre-metastatic niche. Nature *438*, 820–827.

Karnezis, A.N., Cho, K.R., Gilks, C.B., Pearce, C.L., and Huntsman, D.G. (2016). The disparate origins of ovarian cancers: pathogenesis and prevention strategies. Nat. Rev. Cancer *17*, 65–74.

Karnoub, A.E., Dash, A.B., Vo, A.P., Sullivan, A., Brooks, M.W., Bell, G.W., Richardson, A.L., Polyak,

K., Tubo, R., and Weinberg, R.A. (2007). Mesenchymal stem cells within tumour stroma promote breast cancer metastasis. Nature *449*, 557–563.

Katsuda, T., Kosaka, N., Takeshita, F., and Ochiya, T. (2013). The therapeutic potential of mesenchymal stem cell-derived extracellular vesicles. Proteomics *13*, 1637–1653.

Kim, E.-K., Kim, H.-J., Yang, Y.-I., Kim, J.T., Choi, M.-Y., Choi, C.S., Kim, K.-H., Lee, J.-H., Jang, W.-H., and Cheong, S.-H. (2013). Endogenous gastric-resident mesenchymal stem cells contribute to formation of cancer stroma and progression of gastric cancer. Korean J. Pathol. *47*, 507–518.

Kindelberger, D.W., Lee, Y., Miron, A., Hirsch, M.S., Feltmate, C., Medeiros, F., Callahan, M.J., Garner, E.O., Gordon, R.W., Birch, C., et al. (2007). Intraepithelial Carcinoma of the Fimbria and Pelvic Serous Carcinoma: Evidence for a Causal Relationship. Am. J. Surg. Pathol. *31*, 161–169.

Ko, S.Y., Barengo, N., Ladanyi, A., Lee, J.-S., Marini, F., Lengyel, E., and Naora, H. (2012). HOXA9 promotes ovarian cancer growth by stimulating cancer-associated fibroblasts. J. Clin. Invest. *122*, 3603–3617.

Kojima, Y., Acar, A., Eaton, E.N., Mellody, K.T., Scheel, C., Ben-Porath, I., Onder, T.T., Wang, Z.C., Richardson, A.L., Weinberg, R.A., et al. (2010). Autocrine TGF- and stromal cell-derived factor-1 (SDF-1) signaling drives the evolution of tumor-promoting mammary stromal myofibroblasts. Proc. Natl. Acad. Sci. *107*, 20009–20014.

Kollet, O., Dar, A., Shivtiel, S., Kalinkovich, A., Lapid, K., Sztainberg, Y., Tesio, M., Samstein, R.M., Goichberg, P., Spiegel, A., et al. (2006). Osteoclasts degrade endosteal components and promote mobilization of hematopoietic progenitor cells. Nat. Med. *12*, 657–664.

Kopen, G.C., Prockop, D.J., and Phinney, D.G. (1999). Marrow stromal cells migrate throughout forebrain and cerebellum, and they differentiate into astrocytes after injection into neonatal mouse brains. Proc. Natl. Acad. Sci. U. S. A. *96*, 10711–10716.

Krosl, J., Austin, P., Beslu, N., Kroon, E., Humphries, R.K., and Sauvageau, G. (2003). In vitro expansion of hematopoietic stem cells by recombinant TAT-HOXB4 protein. Nat. Med. *9*, 1428–1432.

Kryczek, I., Lange, A., Mottram, P., Alvarez, X., Cheng, P., Hogan, M., Moons, L., Wei, S., Zou, L.,

Machelon, V., et al. (2005). CXCL12 and vascular endothelial growth factor synergistically induce neoangiogenesis in human ovarian cancers. Cancer Res. *65*, 465–472.

Kucerova, L., Matuskova, M., Hlubinova, K., Altanerova, V., and Altaner, C. (2010). Tumor cell behaviour modulation by mesenchymal stromal cells. Mol. Cancer *9*, 129.

Kukreja, P., Abdel-Mageed, A.B., Mondal, D., Liu, K., and Agrawal, K.C. (2005). Up-regulation of CXCR4 Expression in PC-3 Cells by Stromal-Derived Factor-1α (CXCL12) Increases Endothelial Adhesion and Transendothelial Migration: Role of MEK/ERK Signaling Pathway–Dependent NF-κB Activation. Cancer Res. *65*, 9891–9898.

Kunita, A., Kashima, T.G., Ohazama, A., Grigoriadis, A.E., and Fukayama, M. (2011). Podoplanin Is Regulated by AP-1 and Promotes Platelet Aggregation and Cell Migration in Osteosarcoma. Am. J. Pathol. *179*, 1041–1049.

Kurman, R.J., and Shih, I.-M. (2010). The origin and pathogenesis of epithelial ovarian cancer: a proposed unifying theory. Am. J. Surg. Pathol. *34*, 433–443.

Kurman, R.J., and Shih, I.-M. (2011). Molecular pathogenesis and extraovarian origin of epithelial ovarian cancer—Shifting the paradigm. Hum. Pathol. *42*, 918–931.

Lacerda, L., Debeb, B.G., Smith, D., Larson, R., Solley, T., Xu, W., Krishnamurthy, S., Gong, Y., Levy, L.B., Buchholz, T., et al. (2015). Mesenchymal stem cells mediate the clinical phenotype of inflammatory breast cancer in a preclinical model. Breast Cancer Res. *17*, 42.

Lee, R.H., Kim, B., Choi, I., Kim, H., Choi, H.S., Suh, K., Bae, Y.C., and Jung, J.S. (2004). Characterization and Expression Analysis of Mesenchymal Stem Cells from Human Bone Marrow and Adipose Tissue. Cell. Physiol. Biochem. *14*, 311–324.

Lee, Y., Miron, A., Drapkin, R., Nucci, M., Medeiros, F., Saleemuddin, A., Garber, J., Birch, C., Mou, H., Gordon, R., et al. (2007). A candidate precursor to serous carcinoma that originates in the distal fallopian tube. J. Pathol. *211*, 26–35.

Li, Q. (2014). Transforming growth factor β signaling in uterine development and function. J. Anim. Sci. Biotechnol. *5*, 52.

Li, W., Zhou, Y., Yang, J., Zhang, X., Zhang, H., Zhang, T., Zhao, S., Zheng, P., Huo, J., and Wu, H. (2015). Gastric cancer-derived mesenchymal stem cells prompt gastric cancer progression through secretion of interleukin-8. J. Exp. Clin. Cancer Res. *34*, 52.

Linde, N., Fluegen, G., and Aguirre-Ghiso, J.A. (2016). The Relationship Between Dormant Cancer Cells and Their Microenvironment. In Advances in Cancer Research, pp. 45–71.

Lis, R., Touboul, C., Raynaud, C.M., Malek, J.A., Suhre, K., Mirshahi, M., and Rafii, A. (2012). Mesenchymal Cell Interaction with Ovarian Cancer Cells Triggers Pro-Metastatic Properties. PLoS One *7*, e38340.

de Lourdes Mora-García, M., García-Rocha, R., Morales-Ramírez, O., Montesinos, J.J., Weiss-Steider, B., Hernández-Montes, J., Ávila-Ibarra, L.R., Don-López, C.A., Velasco-Velázquez, M.A., Gutiérrez-Serrano, V., et al. (2016). Mesenchymal stromal cells derived from cervical cancer produce high amounts of adenosine to suppress cytotoxic T lymphocyte functions. J. Transl. Med. *14*, 302.

Lowry, K.P., and Lee, S.I. (2017). Imaging and Screening of Ovarian Cancer. Radiol. Clin. North Am. *55*, 1251–1259.

Mantovani, A., Sozzani, S., Locati, M., Allavena, P., and Sica, A. (2002). Macrophage polarization: tumor-associated macrophages as a paradigm for polarized M2 mononuclear phagocytes. Trends Immunol. *23*, 549–555.

Marcato, P., Dean, C.A., Liu, R.-Z., Coyle, K.M., Bydoun, M., Wallace, M., Clements, D., Turner, C., Mathenge, E.G., Gujar, S.A., et al. (2015). Aldehyde dehydrogenase 1A3 influences breast cancer progression via differential retinoic acid signaling. Mol. Oncol. *9*, 17–31.

Martin-Villar, E., Megias, D., Castel, S., Yurrita, M.M., Vilaro, S., and Quintanilla, M. (2006). Podoplanin binds ERM proteins to activate RhoA and promote epithelial-mesenchymal transition. J. Cell Sci. *119*, 4541–4553.

Matulonis, U.A., Sood, A.K., Fallowfield, L., Howitt, B.E., Sehouli, J., and Karlan, B.Y. (2016). Ovarian cancer. Nat. Rev. Dis. Prim. *2*, 16061.

Maurano, M.T., Wang, H., John, S., Canfield, T., Lee, K., Stamatoyannopoulos, J.A., and Shafer, A.

(2015). Role of DNA Methylation in Modulating Transcription Factor Occupancy. CellReports *12*, 1184–1195.

McDaniel, A.S., Stall, J.N., Hovelson, D.H., Cani, A.K., Liu, C.-J., Tomlins, S.A., and Cho, K.R. (2015). Next-Generation Sequencing of Tubal Intraepithelial Carcinomas. JAMA Oncol. *1*, 1128–1132.

McLean, K., Gong, Y., Choi, Y., Deng, N., Yang, K., Bai, S., Cabrera, L., Keller, E., McCauley, L., Cho, K.R., et al. (2011). Human ovarian carcinoma–associated mesenchymal stem cells regulate cancer stem cells and tumorigenesis via altered BMP production. J. Clin. Invest. *121*, 3206–3219.

Medeiros, F., Muto, M.G., Lee, Y., Elvin, J.A., Callahan, M.J., Feltmate, C., Garber, J.E., Cramer, D.W., and Crum, C.P. (2006). The tubal fimbria is a preferred site for early adenocarcinoma in women with familial ovarian cancer syndrome. Am. J. Surg. Pathol. *30*, 230–236.

Meert, A.-P., Paesmans, M., Martin, B., Delmotte, P., Berghmans, T., Verdebout, J.-M., Lafitte, J.-J., Mascaux, C., and Sculier, J.-P. (2002). The role of microvessel density on the survival of patients with lung cancer: a systematic review of the literature with meta-analysis. Br. J. Cancer *87*, 694–701.

Meinhold-Heerlein, I., and Hauptmann, S. (2014). The heterogeneity of ovarian cancer. Arch. Gynecol. Obstet. *289*, 237–239.

Mishra, P.J., Mishra, P.J., Humeniuk, R., Medina, D.J., Alexe, G., Mesirov, J.P., Ganesan, S., Glod, J.W., and Banerjee, D. (2008). Carcinoma-Associated Fibroblast-Like Differentiation of Human Mesenchymal Stem Cells. Cancer Res. *68*, 4331–4339.

Morrison, J.C., Blanco, L.Z., Vang, R., and Ronnett, B.M. (2015). Incidental Serous Tubal Intraepithelial Carcinoma and Early Invasive Serous Carcinoma in the Nonprophylactic Setting. Am. J. Surg. Pathol. *39*, 442–453.

Motz, G.T., and Coukos, G. (2011). The parallel lives of angiogenesis and immunosuppression: cancer and other tales. Nat. Rev. Immunol. *11*, 702–711.

Nabha, S.M., dos Santos, E.B., Yamamoto, H.A., Belizi, A., Dong, Z., Meng, H., Saliganan, A., Sabbota, A., Bonfil, R.D., and Cher, M.L. (2008). Bone marrow stromal cells enhance prostate cancer cell invasion through type I collagen in an MMP-12 dependent manner. Int. J. Cancer *122*, 2482–2490.

Najmi, S., Korah, R., Chandra, R., Abdellatif, M., and Wieder, R. (2005). Flavopiridol Blocks Integrin-Mediated Survival in Dormant Breast Cancer Cells. Clin. Cancer Res. *11*, 2038–2046.

Nelson, B.H. (2010). CD20+ B Cells: The Other Tumor-Infiltrating Lymphocytes. J. Immunol. *185*, 4977–4982.

Orimo, A., Gupta, P.B., Sgroi, D.C., Arenzana-Seisdedos, F., Delaunay, T., Naeem, R., Carey, V.J., Richardson, A.L., and Weinberg, R.A. (2005). Stromal Fibroblasts Present in Invasive Human Breast Carcinomas Promote Tumor Growth and Angiogenesis through Elevated SDF-1/CXCL12 Secretion. Cell *121*, 335–348.

Ortiz, L.A., Gambelli, F., McBride, C., Gaupp, D., Baddoo, M., Kaminski, N., and Phinney, D.G. (2003). Mesenchymal stem cell engraftment in lung is enhanced in response to bleomycin exposure and ameliorates its fibrotic effects. Proc. Natl. Acad. Sci. *100*, 8407–8411.

Otsu, K., Das, S., Houser, S.D., Quadri, S.K., Bhattacharya, S., and Bhattacharya, J. (2009). Concentration-dependent inhibition of angiogenesis by mesenchymal stem cells. Blood *113*, 4197–4205.

Pardoll, D.M. (2012). The blockade of immune checkpoints in cancer immunotherapy. Nat. Rev. Cancer *12*, 252–264.

Paunescu, V., Bojin, F.M., Tatu, C.A., Gavriliuc, O.I., Rosca, A., Gruia, A.T., Tanasie, G., Bunu, C., Crisnic, D., Gherghiceanu, M., et al. (2011). Tumour-associated fibroblasts and mesenchymal stem cells: more similarities than differences. J. Cell. Mol. Med. *15*, 635–646.

Peng, S.-B., Peek, V., Zhai, Y., Paul, D.C., Lou, Q., Xia, X., Eessalu, T., Kohn, W., and Tang, S. (2005). Akt activation, but not extracellular signal-regulated kinase activation, is required for SDF-1alpha/CXCR4-mediated migration of epitheloid carcinoma cells. Mol. Cancer Res. *3*, 227–236.

Perets, R., Wyant, G.A., Muto, K.W., Bijron, J.G., Poole, B.B., Chin, K.T., Chen, J.Y.H., Ohman, A.W., Stepule, C.D., Kwak, S., et al. (2013). Transformation of the fallopian tube secretory epithelium leads to high-grade serous ovarian cancer in Brca;Tp53;Pten models. Cancer Cell *24*, 751–765.

Pietras, K., and Östman, A. (2010). Hallmarks of cancer: Interactions with the tumor stroma. Exp. Cell Res. *316*, 1324–1331.

Pittenger, M.F., Mackay, A.M., Beck, S.C., Jaiswal, R.K., Douglas, R., Mosca, J.D., Moorman, M.A., Simonetti, D.W., Craig, S., and Marshak, D.R. (1999). Multilineage potential of adult human mesenchymal stem cells. Science *284*, 143–147.

Polanska, U.M., and Orimo, A. (2013). Carcinoma-associated fibroblasts: Non-neoplastic tumour-promoting mesenchymal cells. J. Cell. Physiol. *228*, 1651–1657.

Pollard, J.W. (2004). Opinion: Tumour-educated macrophages promote tumour progression and metastasis. Nat. Rev. Cancer *4*, 71–78.

Porcile, C., Bajetto, A., Barbieri, F., Barbero, S., Bonavia, R., Biglieri, M., Pirani, P., Florio, T., and Schettini, G. (2005). Stromal cell-derived factor-1α (SDF-1α/CXCL12) stimulates ovarian cancer cell growth through the EGF receptor transactivation. Exp. Cell Res. *308*, 241–253.

Prantl, L., Muehlberg, F., Navone, N.M., Song, Y.-H., Vykoukal, J., Logothetis, C.J., and Alt, E.U. (2010a). Adipose tissue-derived stem cells promote prostate tumor growth. Prostate *70*, 1709–1715.

Prantl, L., Muehlberg, F., Navone, N.M., Song, Y.-H., Vykoukal, J., Logothetis, C.J., and Alt, E.U. (2010b). Adipose tissue-derived stem cells promote prostate tumor growth. Prostate *70*, 1709–1715.

Psaila, B., and Lyden, D. (2009). The metastatic niche: adapting the foreign soil. Nat. Rev. Cancer *9*, 285–293.

Pylayeva-Gupta, Y., Lee, K.E., Hajdu, C.H., Miller, G., and Bar-Sagi, D. (2012). Oncogenic Kras-Induced GM-CSF Production Promotes the Development of Pancreatic Neoplasia. Cancer Cell *21*, 836–847.

Quante, M., Tu, S.P., Tomita, H., Gonda, T., Wang, S.S.W., Takashi, S., Baik, G.H., Shibata, W., Diprete, B., Betz, K.S., et al. (2011). Bone marrow-derived myofibroblasts contribute to the mesenchymal stem cell niche and promote tumor growth. Cancer Cell *19*, 257–272.

Rabban, J.T., Vohra, P., and Zaloudek, C.J. (2015). Nongynecologic Metastases to Fallopian Tube Mucosa. Am. J. Surg. Pathol. *39*, 35–51.

Rauh-Hain, J.A., Krivak, T.C., Del Carmen, M.G., and Olawaiye, A.B. (2011). Ovarian cancer screening

and early detection in the general population. Rev. Obstet. Gynecol. *4*, 15–21.

Ravi, M., Paramesh, V., Kaviya, S.R., Anuradha, E., and Solomon, F.D.P. (2015). 3D Cell Culture Systems: Advantages and Applications. J. Cell. Physiol. *230*, 16–26.

Reyes, C., Murali, R., and Park, K.J. (2015). Secondary Involvement of the Adnexa and Uterine Corpus by Carcinomas of the Uterine Cervix. Int. J. Gynecol. Pathol. *34*, 551–563.

Rhim, A.D., Oberstein, P.E., Thomas, D.H., Mirek, E.T., Palermo, C.F., Sastra, S.A., Dekleva, E.N., Saunders, T., Becerra, C.P., Tattersall, I.W., et al. (2014). Stromal elements act to restrain, rather than support, pancreatic ductal adenocarcinoma. Cancer Cell *25*, 735–747.

Ridge, S.M., Sullivan, F.J., and Glynn, S.A. (2017). Mesenchymal stem cells: key players in cancer progression. Mol. Cancer *16*, 31.

Riekstina, U., Cakstina, I., Parfejevs, V., Hoogduijn, M., Jankovskis, G., Muiznieks, I., Muceniece, R., and Ancans, J. (2009). Embryonic Stem Cell Marker Expression Pattern in Human Mesenchymal Stem Cells Derived from Bone Marrow, Adipose Tissue, Heart and Dermis. Stem Cell Rev. Reports *5*, 378–386.

Ritchie, M.E., Phipson, B., Wu, D., Hu, Y., Law, C.W., Shi, W., and Smyth, G.K. (2015). limma powers differential expression analyses for RNA-sequencing and microarray studies. Nucleic Acids Res. *43*, e47–e47.

Robinson, M.D., McCarthy, D.J., and Smyth, G.K. (2010). edgeR: a Bioconductor package for differential expression analysis of digital gene expression data. Bioinformatics *26*, 139–140.

Rodriguez-Torres, M., and Allan, A.L. (2016). Aldehyde dehydrogenase as a marker and functional mediator of metastasis in solid tumors. Clin. Exp. Metastasis *33*, 97–113.

Rotem, A., Janzer, A., Izar, B., Ji, Z., Doench, J.G., Garraway, L.A., and Struhl, K. (2015). Alternative to the soft-agar assay that permits high-throughput drug and genetic screens for cellular transformation. Proc. Natl. Acad. Sci. U. S. A. *112*, 5708–5713.

Ruppender, N., Larson, S., Lakely, B., Kollath, L., Brown, L., Coleman, I., Coleman, R., Nguyen, H.,

Nelson, P.S., Corey, E., et al. (2015). Cellular Adhesion Promotes Prostate Cancer Cells Escape from Dormancy. PLoS One *10*, e0130565.

Ruster, B., Gottig, S., Ludwig, R.J., Bistrian, R., Muller, S., Seifried, E., Gille, J., and Henschler, R. (2006). Mesenchymal stem cells display coordinated rolling and adhesion behavior on endothelial cells. Blood *108*, 3938–3944.

Sart, S., Tsai, A.-C., Li, Y., and Ma, T. (2014). Three-dimensional aggregates of mesenchymal stem cells: cellular mechanisms, biological properties, and applications. Tissue Eng. Part B. Rev. *20*, 365–380.

Sato, T., Sakai, T., Noguchi, Y., Takita, M., Hirakawa, S., and Ito, A. (2004). Tumor-stromal cell contact promotes invasion of human uterine cervical carcinoma cells by augmenting the expression and activation of stromal matrix metalloproteinases. Gynecol. Oncol. *92*, 47–56.

Sato, Y., Araki, H., Kato, J., Nakamura, K., Kawano, Y., Kobune, M., Sato, T., Miyanishi, K., Takayama, T., Takahashi, M., et al. (2005). Human mesenchymal stem cells xenografted directly to rat liver are differentiated into human hepatocytes without fusion. Blood *106*, 756–763.

Schauer, I.G., Zhang, J., Xing, Z., Guo, X., Mercado-Uribe, I., Sood, A.K., Huang, P., and Liu, J. (2013a). Interleukin-1β promotes ovarian tumorigenesis through a p53/NF-κB-mediated inflammatory response in stromal fibroblasts. Neoplasia *15*, 409–420.

Schauer, I.G., Zhang, J., Xing, Z., Guo, X., Mercado-Uribe, I., Sood, A.K., Huang, P., and Liu, J. (2013b). Interleukin-1β promotes ovarian tumorigenesis through a p53/NF-κB-mediated inflammatory response in stromal fibroblasts. Neoplasia *15*, 409–420.

Scholl, F.G., Gamallo, C., Vilaró, S., and Quintanilla, M. (1999). Identification of PA2.26 antigen as a novel cell-surface mucin-type glycoprotein that induces plasma membrane extensions and increased motility in keratinocytes. J. Cell Sci. *112 (Pt 24)*, 4601–4613.

Scotton, C.J., Wilson, J.L., Scott, K., Stamp, G., Wilbanks, G.D., Fricker, S., Bridger, G., and Balkwill, F.R. (2002). Multiple actions of the chemokine CXCL12 on epithelial tumor cells in human ovarian cancer. Cancer Res. *62*, 5930–5938.

Serrano, M., Lin, A.W., McCurrach, M.E., Beach, D., and Lowe, S.W. (1997). Oncogenic ras provokes premature cell senescence associated with accumulation of p53 and p16INK4a. Cell *88*, 593–602.

Shangguan, L., Ti, X., Krause, U., Hai, B., Zhao, Y., Yang, Z., and Liu, F. (2012). Inhibition of TGF-β/Smad Signaling by BAMBI Blocks Differentiation of Human Mesenchymal Stem Cells to Carcinoma-Associated Fibroblasts and Abolishes their Protumor Effects. Stem Cells *30*, 2810–2819.

Shojaei, F., Wu, X., Qu, X., Kowanetz, M., Yu, L., Tan, M., Meng, Y.G., and Ferrara, N. (2009). G-CSF-initiated myeloid cell mobilization and angiogenesis mediate tumor refractoriness to anti-VEGF therapy in mouse models. Proc. Natl. Acad. Sci. U. S. A. *106*, 6742–6747.

Sica, A., Schioppa, T., Mantovani, A., and Allavena, P. (2006). Tumour-associated macrophages are a distinct M2 polarised population promoting tumour progression: Potential targets of anti-cancer therapy. Eur. J. Cancer *42*, 717–727.

Siegel, R.L., Miller, K.D., and Jemal, A. (2017). Cancer statistics, 2017. CA. Cancer J. Clin. *67*, 7–30.

Sosa, M.S., Avivar-Valderas, A., Bragado, P., Wen, H.-C., and Aguirre-Ghiso, J.A. (2011). ERK1/2 and p38α/β signaling in tumor cell quiescence: opportunities to control dormant residual disease. Clin. Cancer Res. *17*, 5850–5857.

Sosa, M.S., Bragado, P., and Aguirre-Ghiso, J.A. (2014). Mechanisms of disseminated cancer cell dormancy: an awakening field. Nat. Rev. Cancer *14*, 611–622.

Spaeth, E.L., Dembinski, J.L., Sasser, A.K., Watson, K., Klopp, A., Hall, B., Andreeff, M., and Marini, F. (2009). Mesenchymal Stem Cell Transition to Tumor-Associated Fibroblasts Contributes to Fibrovascular Network Expansion and Tumor Progression. PLoS One *4*, e4992.

Stegner, D., Dütting, S., and Nieswandt, B. (2014). Mechanistic explanation for platelet contribution to cancer metastasis. Thromb. Res. *133*, S149–S157.

Strilic, B., and Offermanns, S. (2017). Intravascular Survival and Extravasation of Tumor Cells. Cancer Cell *32*, 282–293.

Subramanian, A., Tamayo, P., Mootha, V.K., Mukherjee, S., Ebert, B.L., Gillette, M.A., Paulovich, A.,

Pomeroy, S.L., Golub, T.R., Lander, E.S., et al. (2005). Gene set enrichment analysis: a knowledge-based approach for interpreting genome-wide expression profiles. Proc. Natl. Acad. Sci. U. S. A. *102*, 15545–15550.

Sun, B., Roh, K.-H., Park, J.-R., Lee, S.-R., Park, S.-B., Jung, J.-W., Kang, S.-K., Lee, Y.-S., and Kang, K.-S. (2009). Therapeutic potential of mesenchymal stromal cells in a mouse breast cancer metastasis model. Cytotherapy *11*, 289–298.

Sun, Z., Wang, S., and Zhao, R. (2014). The roles of mesenchymal stem cells in tumor inflammatory microenvironment. J. Hematol. Oncol. *7*, 14.

Sung, S.-Y., Hsieh, C.-L., Law, A., Zhau, H.E., Pathak, S., Multani, A.S., Lim, S., Coleman, I.M., Wu, L.-C., Figg, W.D., et al. (2008). Coevolution of Prostate Cancer and Bone Stroma in Three-Dimensional Coculture: Implications for Cancer Growth and Metastasis. Cancer Res. *68*, 9996–10003.

Suzuki, K., Sun, R., Origuchi, M., Kanehira, M., Takahata, T., Itoh, J., Umezawa, A., Kijima, H., Fukuda, S., and Saijo, Y. (2011). Mesenchymal stromal cells promote tumor growth through the enhancement of neovascularization. Mol. Med. *17*, 579–587.

Takeuchi, S., Fukuda, K., Yamada, T., Arai, S., Takagi, S., Ishii, G., Ochiai, A., Iwakiri, S., Itoi, K., Uehara, H., et al. (2017). Podoplanin promotes progression of malignant pleural mesothelioma by regulating motility and focus formation. Cancer Sci. *108*, 696–703.

Terada, K.Y., Ahn, H.J., and Kessel, B. (2016). Differences in risk for type 1 and type 2 ovarian cancer in a large cancer screening trial. J. Gynecol. Oncol. *27*, e25.

Tomchuck, S.L., Zwezdaryk, K.J., Coffelt, S.B., Waterman, R.S., Danka, E.S., and Scandurro, A.B. (2008). Toll-Like Receptors on Human Mesenchymal Stem Cells Drive Their Migration and Immunomodulating Responses. Stem Cells *26*, 99–107.

Tone, A.A., Salvador, S., Finlayson, S.J., Tinker, A. V, Kwon, J.S., Lee, C.-H., Cohen, T., Ehlen, T., Lee, M., Carey, M.S., et al. (2012). The role of the fallopian tube in ovarian cancer. Clin. Adv. Hematol. Oncol. *10*, 296–306.

Touboul, C., Vidal, F., Pasquier, J., Lis, R., and Rafii, A. (2014). Role of mesenchymal cells in the natural

history of ovarian cancer: a review. J. Transl. Med. *12*, 271.

Uzzan, B., Nicolas, P., Cucherat, M., and Perret, G.-Y. (2004). Microvessel density as a prognostic factor in women with breast cancer: a systematic review of the literature and meta-analysis. Cancer Res. *64*, 2941–2955.

Verardo, R., Piazza, S., Klaric, E., Ciani, Y., Bussadori, G., Marzinotto, S., Mariuzzi, L., Cesselli, D., Beltrami, A.P., Mano, M., et al. (2014). Specific Mesothelial Signature Marks the Heterogeneity of Mesenchymal Stem Cells From High-Grade Serous Ovarian Cancer. Stem Cells *32*, 2998–3011.

Veres, D. V., Gyurkó, D.M., Thaler, B., Szalay, K.Z., Fazekas, D., Korcsmáros, T., and Csermely, P. (2015). ComPPI: a cellular compartment-specific database for protein–protein interaction network analysis. Nucleic Acids Res. *43*, D485–D493.

Vihinen, P., and Kähäri, V.-M. (2002). Matrix metalloproteinases in cancer: Prognostic markers and therapeutic targets. Int. J. Cancer *99*, 157–166.

de Visser, K.E., Korets, L. V., and Coussens, L.M. (2005). De novo carcinogenesis promoted by chronic inflammation is B lymphocyte dependent. Cancer Cell *7*, 411–423.

Wagner, W., Wein, F., Seckinger, A., Frankhauser, M., Wirkner, U., Krause, U., Blake, J., Schwager, C., Eckstein, V., Ansorge, W., et al. (2005). Comparative characteristics of mesenchymal stem cells from human bone marrow, adipose tissue, and umbilical cord blood. Exp. Hematol. *33*, 1402–1416.

Wakitani, S., Saito, T., and Caplan, A.I. (1995). Myogenic cells derived from rat bone marrow mesenchymal stem cells exposed to 5-azacytidine. Muscle Nerve *18*, 1417–1426.

Watanabe, T., Hashimoto, T., Sugino, T., Soeda, S., Nishiyama, H., Morimura, Y., Yamada, H., Goodison, S., and Fujimori, K. (2012). Production of IL1-beta by ovarian cancer cells induces mesothelial cell beta1-integrin expression facilitating peritoneal dissemination. J. Ovarian Res. *5*, 7.

Waterman, R.S., Tomchuck, S.L., Henkle, S.L., and Betancourt, A.M. (2010). A New Mesenchymal Stem Cell (MSC) Paradigm: Polarization into a Pro-Inflammatory MSC1 or an Immunosuppressive MSC2 Phenotype. PLoS One *5*, e10088.

Waterman, R.S., Henkle, S.L., and Betancourt, A.M. (2012). Mesenchymal Stem Cell 1 (MSC1)-Based Therapy Attenuates Tumor Growth Whereas MSC2-Treatment Promotes Tumor Growth and Metastasis. PLoS One *7*, e45590.

Weidle, U.H., Birzele, F., Kollmorgen, G., and Rüger, R. (2016). Molecular Mechanisms of Bone Metastasis. Cancer Genomics Proteomics *13*, 1–12.

Wicki, A., Lehembre, F., Wick, N., Hantusch, B., Kerjaschki, D., and Christofori, G. (2006). Tumor invasion in the absence of epithelial-mesenchymal transition: Podoplanin-mediated remodeling of the actin cytoskeleton. Cancer Cell *9*, 261–272.

Willert, K., Brown, J.D., Danenberg, E., Duncan, A.W., Weissman, I.L., Reya, T., Yates, J.R., and Nusse, R. (2003). Wnt proteins are lipid-modified and can act as stem cell growth factors. Nature *423*, 448–452.

Workman, C., Jensen, L.J., Jarmer, H., Berka, R., Gautier, L., Nielser, H.B., Saxild, H.-H., Nielsen, C., Brunak, S., and Knudsen, S. (2002). A new non-linear normalization method for reducing variability in DNA microarray experiments. Genome Biol. *3*, research0048.

Worringer, K.A., Rand, T.A., Hayashi, Y., Sami, S., Takahashi, K., Tanabe, K., Narita, M., Srivastava, D., and Yamanaka, S. (2014). The let-7/LIN-41 pathway regulates reprogramming to human induced pluripotent stem cells by controlling expression of prodifferentiation genes. Cell Stem Cell *14*, 40–52.

Wu, G.D., Nolta, J.A., Jin, Y.-S., Barr, M.L., Yu, H., Starnes, V.A., and Cramer, D. V. (2003). Migration of mesenchymal stem cells to heart allografts during chronic rejection. Transplantation *75*, 679–685.

Wu, Y., Siadaty, M.S., Berens, M.E., Hampton, G.M., and Theodorescu, D. (2008). Overlapping gene expression profiles of cell migration and tumor invasion in human bladder cancer identify metallothionein 1E and nicotinamide N-methyltransferase as novel regulators of cell migration. Oncogene *27*, 6679–6689.

Yamashita, M., Ogawa, T., Zhang, X., Hanamura, N., Kashikura, Y., Takamura, M., Yoneda, M., and Shiraishi, T. (2012). Role of stromal myofibroblasts in invasive breast cancer: stromal expression of alpha-smooth muscle actin correlates with worse clinical outcome. Breast Cancer *19*, 170–176.

Yang, F.-C., Ingram, D.A., Chen, S., Zhu, Y., Yuan, J., Li, X., Yang, X., Knowles, S., Horn, W., Li, Y.,

et al. (2008). Nf1-dependent tumors require a microenvironment containing Nf1+/-- and c-kit-dependent bone marrow. Cell *135*, 437–448.

Ye, H., Cheng, J., Tang, Y., Liu, Z., Xu, C., Liu, Y., and Sun, Y. (2012). Human Bone Marrow-Derived Mesenchymal Stem Cells produced TGFbeta Contributes to Progression and Metastasis of Prostate Cancer. Cancer Invest. *30*, 513–518.

Yeung, T.-L., Leung, C.S., Wong, K.-K., Samimi, G., Thompson, M.S., Liu, J., Zaid, T.M., Ghosh, S., Birrer, M.J., and Mok, S.C. (2013). TGF- Modulates Ovarian Cancer Invasion by Upregulating CAF-Derived Versican in the Tumor Microenvironment. Cancer Res. *73*, 5016–5028.

Young, M.R., and Wright, M.A. (1992). Myelopoiesis-associated immune suppressor cells in mice bearing metastatic Lewis lung carcinoma tumors: gamma interferon plus tumor necrosis factor alpha synergistically reduces immune suppressor and tumor growth-promoting activities of bone marrow cells and diminishes tumor recurrence and metastasis. Cancer Res. *52*, 6335–6340.

Yu, L.-X., Yan, L., Yang, W., Wu, F.-Q., Ling, Y., Chen, S.-Z., Tang, L., Tan, Y.-X., Cao, D., Wu, M.-C., et al. (2014). Platelets promote tumour metastasis via interaction between TLR4 and tumour cell-released high-mobility group box1 protein. Nat. Commun. *5*, 5256.

Zeisberg, E.M., Potenta, S., Xie, L., Zeisberg, M., and Kalluri, R. (2007). Discovery of Endothelial to Mesenchymal Transition as a Source for Carcinoma-Associated Fibroblasts. Cancer Res. *67*, 10123–10128.

Zhang, C.C., Kaba, M., Ge, G., Xie, K., Tong, W., Hug, C., and Lodish, H.F. (2006). Angiopoietin-like proteins stimulate ex vivo expansion of hematopoietic stem cells. Nat. Med. *12*, 240–245.

Zhang, J., Niu, C., Ye, L., Huang, H., He, X., Tong, W.-G., Ross, J., Haug, J., Johnson, T., Feng, J.Q., et al. (2003). Identification of the haematopoietic stem cell niche and control of the niche size. Nature *425*, 836–841.

Zhang, S., Royer, R., Li, S., McLaughlin, J.R., Rosen, B., Risch, H.A., Fan, I., Bradley, L., Shaw, P.A., and Narod, S.A. (2011). Frequencies of BRCA1 and BRCA2 mutations among 1,342 unselected patients with invasive ovarian cancer. Gynecol. Oncol. *121*, 353–357.

Zhu, W., Xu, W., Jiang, R., Qian, H., Chen, M., Hu, J., Cao, W., Han, C., and Chen, Y. (2006). Mesenchymal stem cells derived from bone marrow favor tumor cell growth in vivo. Exp. Mol. Pathol. *80*, 267–274.

Zou, W., Machelon, V., Coulomb-L'Hermin, A., Borvak, J., Nome, F., Isaeva, T., Wei, S., Krzysiek, R., Durand-Gasselin, I., Gordon, A., et al. (2001). Stromal-derived factor-1 in human tumors recruits and alters the function of plasmacytoid precursor dendritic cells. Nat. Med. *7*, 1339–1346.